Electronic Supplementary Material (ESI) for Dalton Transactions.

SUPPORTING INFORMATION

Aminopiperidine complexes for lactide polymerisation

Paul McKeown, Matthew G. Davidson, John P. Lowe, Mary F. Mahon, Lynne H. Thomas, Timothy J. Woodman and Matthew D. Jones

Characterisation of ligands and complexes

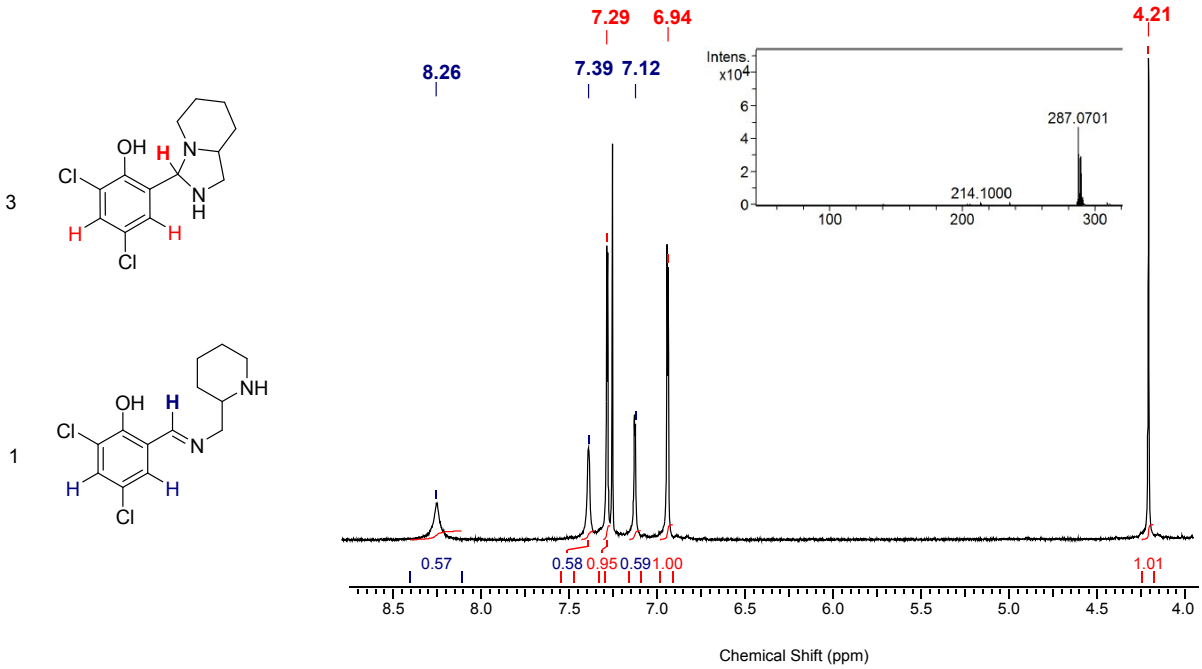

Figure SI1: ^{1}H NMR ($CDCl_3$ 400MHz) spectrum of aromatic region for $\mathbf{1}H_2$ precursor. Inset: ESI-TOF spectrum

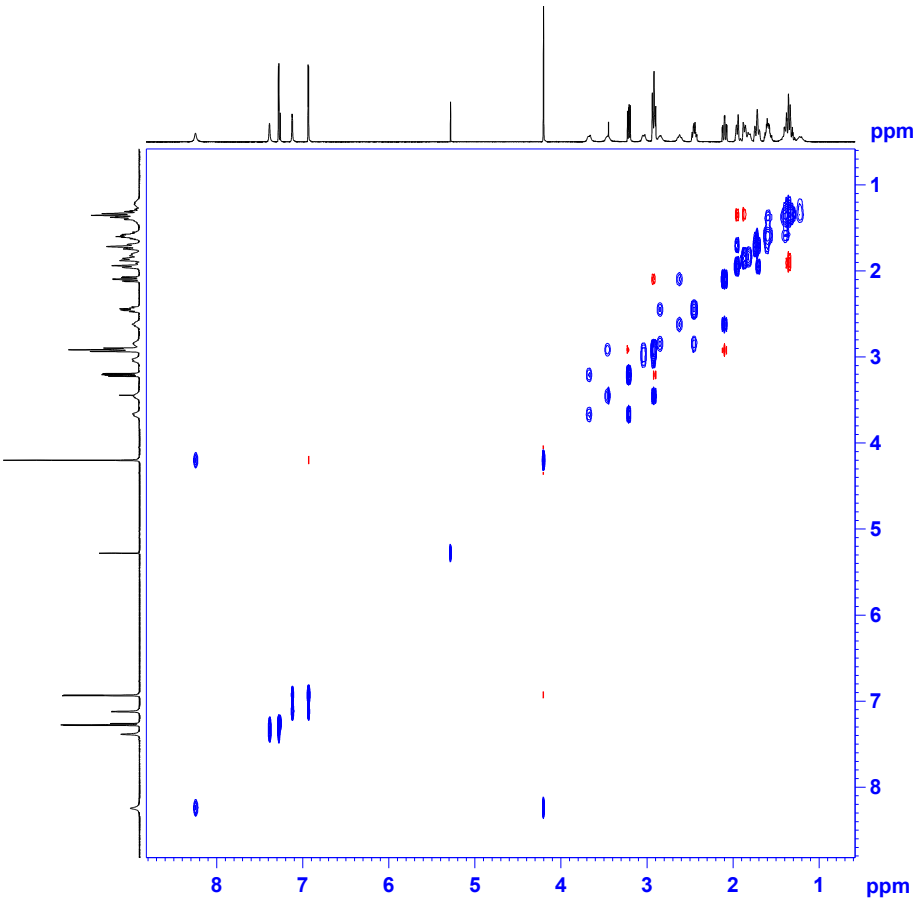

Figure SI2: ^{1}H EXSY NMR ($CDCl_3$, 500 MHz, mixing time 0.6 s) spectrum with blue cross peaks showing chemical exchange and red cross peaks showing NOE.

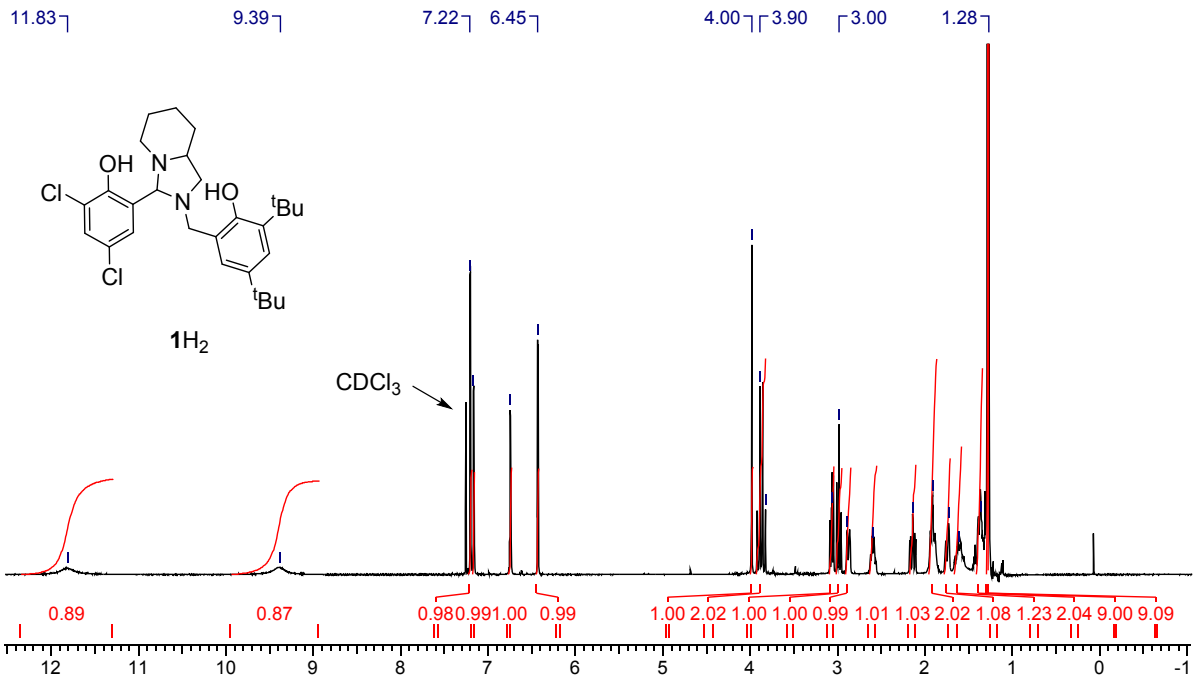

Figure SI3: ^{1}H NMR ($CDCl_3$ 400MHz) spectrum of **1**H_2

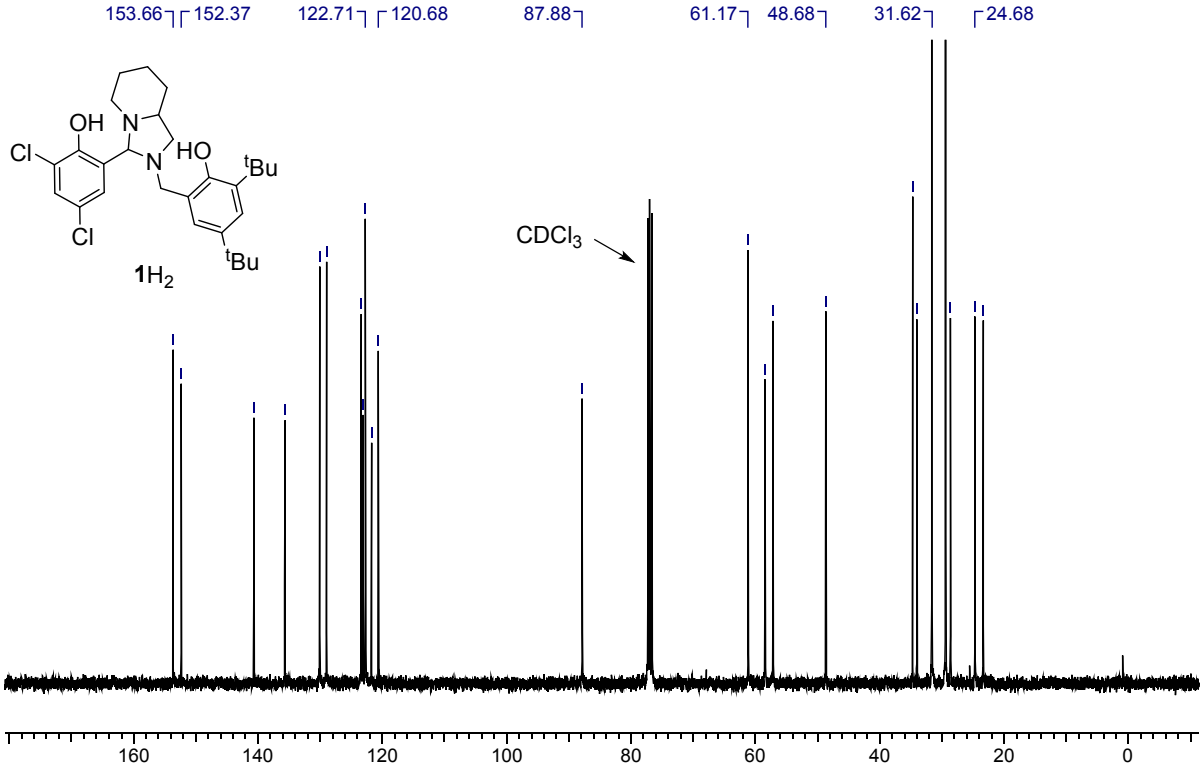

Figure SI4: ^{13}C{^{1}H} NMR ($CDCl_3$, 100MHz) spectrum of **1**H_2

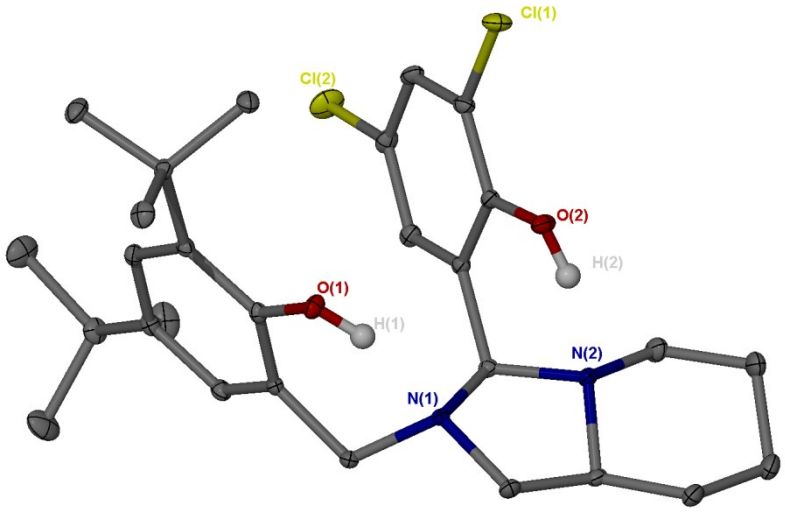

Figure SI5: Solid state structure of **1**H_2. Ellipsoids are shown at the 30% probability level.

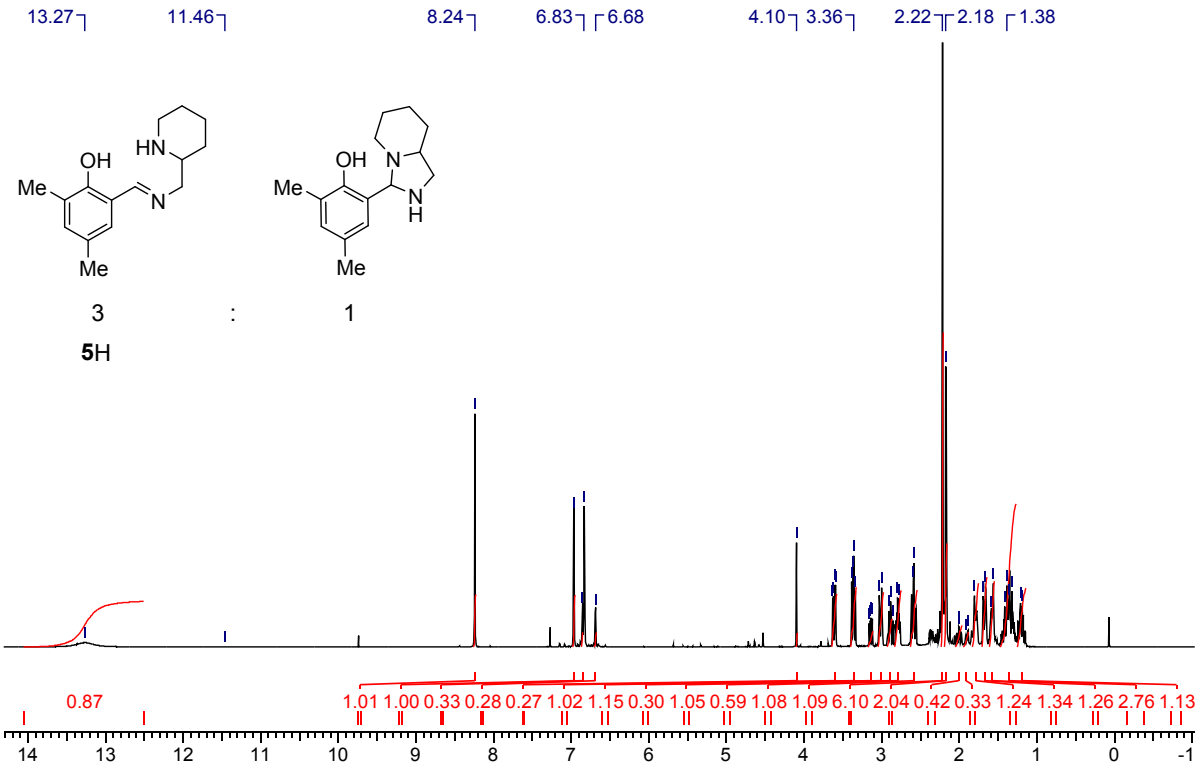

Figure SI6: ^{1}H NMR ($CDCl_3$ 400MHz) spectrum of **5**H.

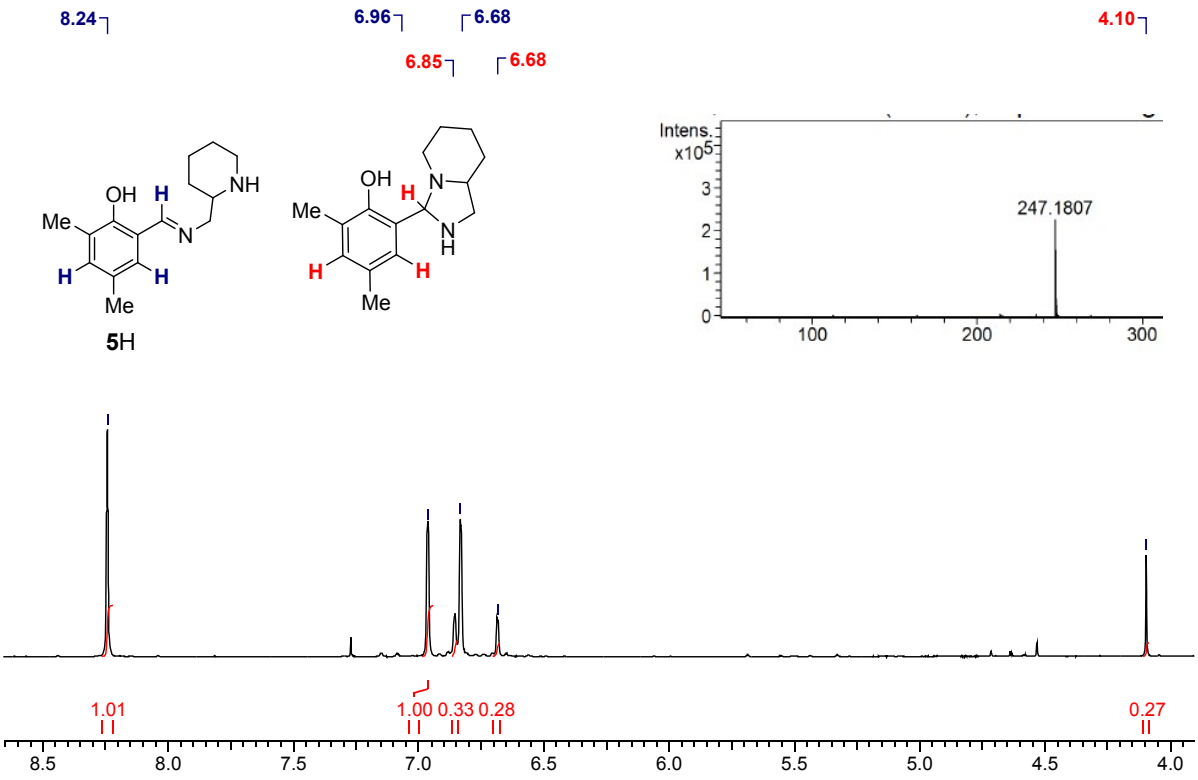

Figure SI7: ^{1}H NMR ($CDCl_3$ 400MHz) spectrum of aromatic region for **5**H; Inset: ESI-TOF spectrum

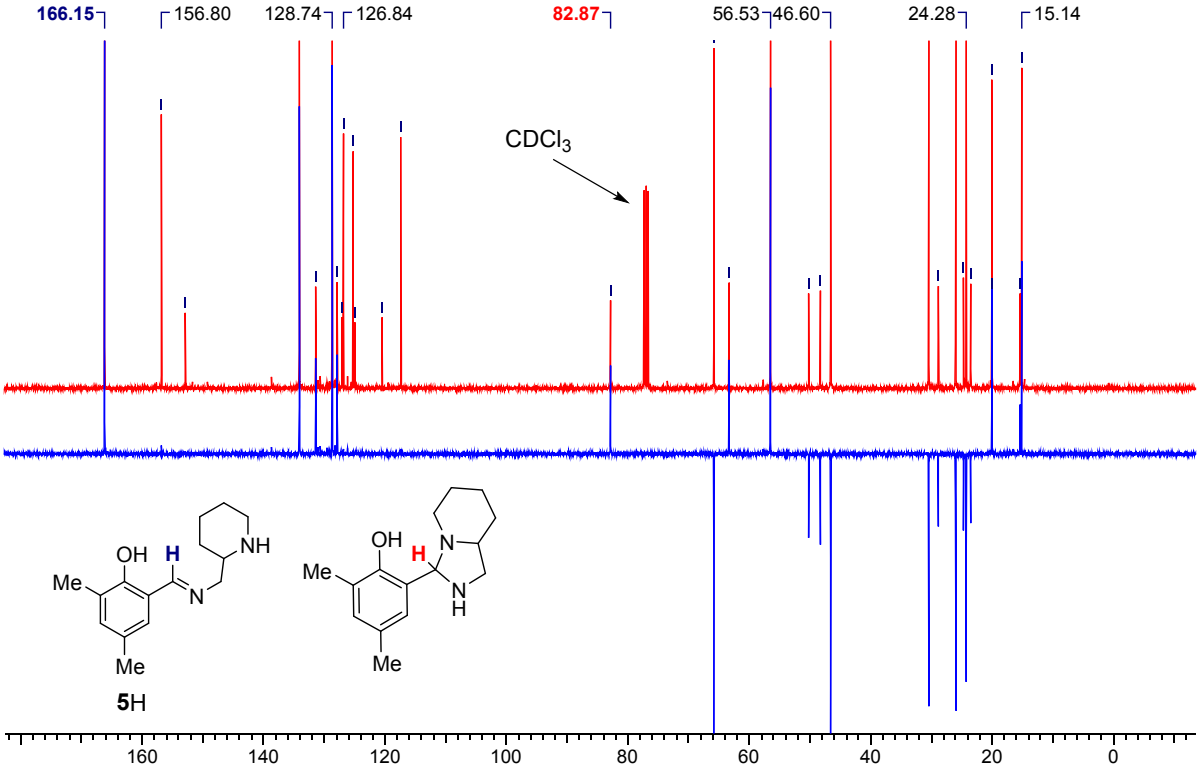

Figure SI8: $^{13}C\{^{1}H\}$ NMR ($CDCl_3$ 100MHz) spectrum (Red) of **5**H with ^{13}C Dept (Blue) overlaid.

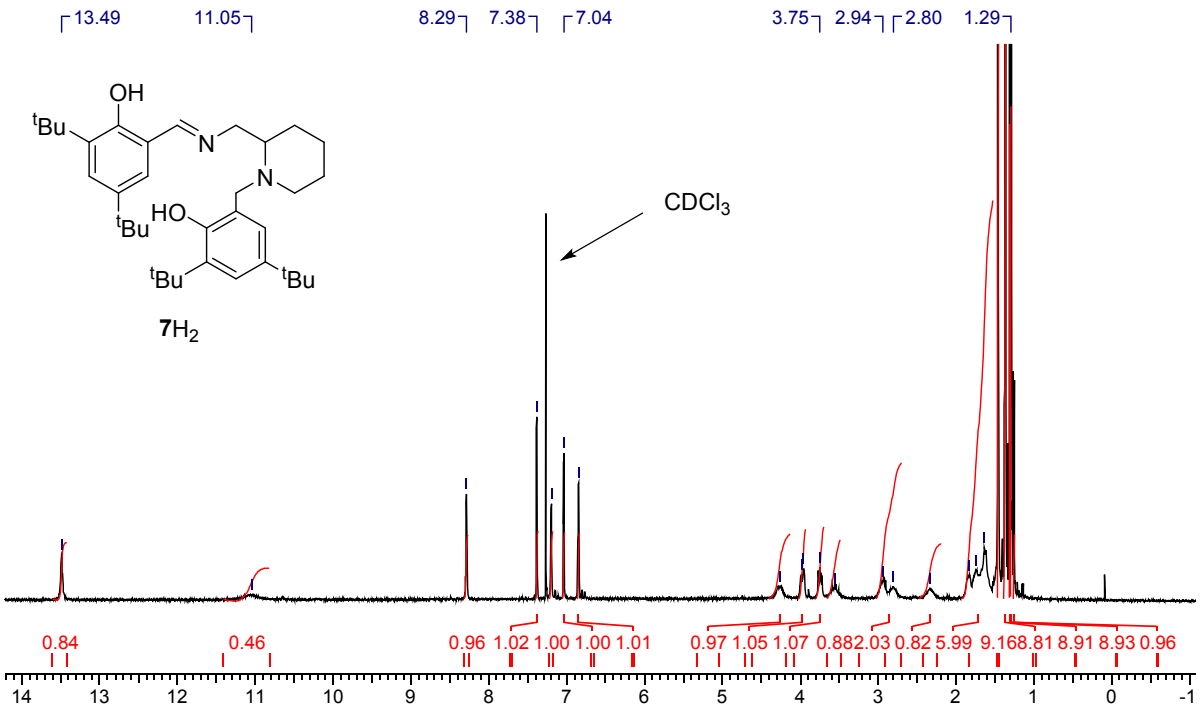

Figure SI9: ^{1}H NMR ($CDCl_3$ 400MHz) spectrum of **7**H_2.

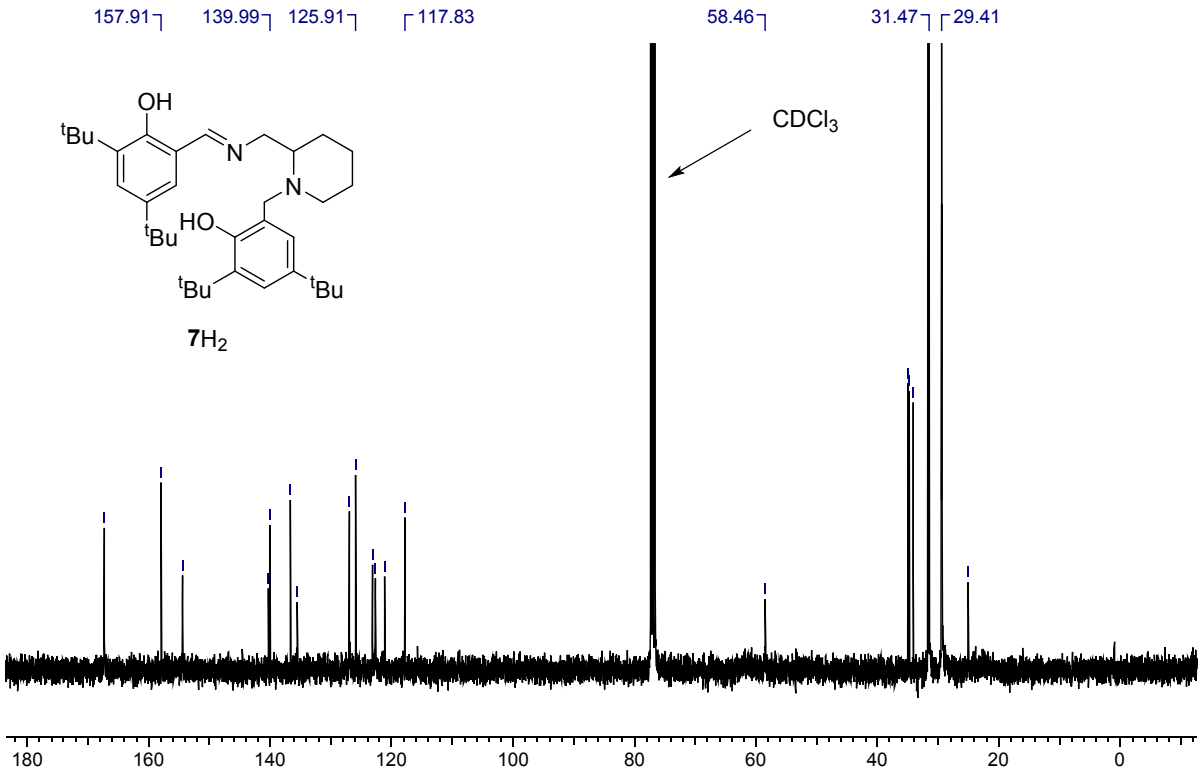

Figure SI10: $^{13}C\{^{1}H\}$ NMR ($CDCl_3$, 100MHz) spectrum of **7**H_2.

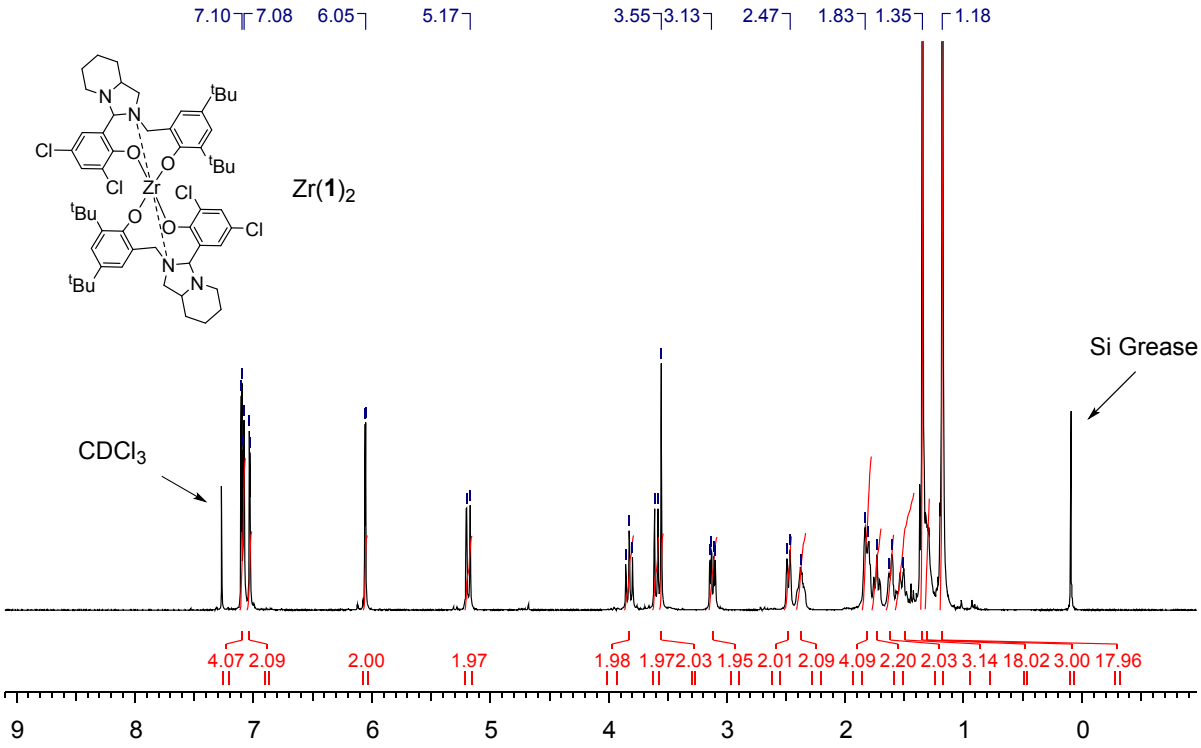

Figure SI11: ^{1}H NMR ($CDCl_3$, 400MHz) spectrum of Zr(**1**)$_2$.

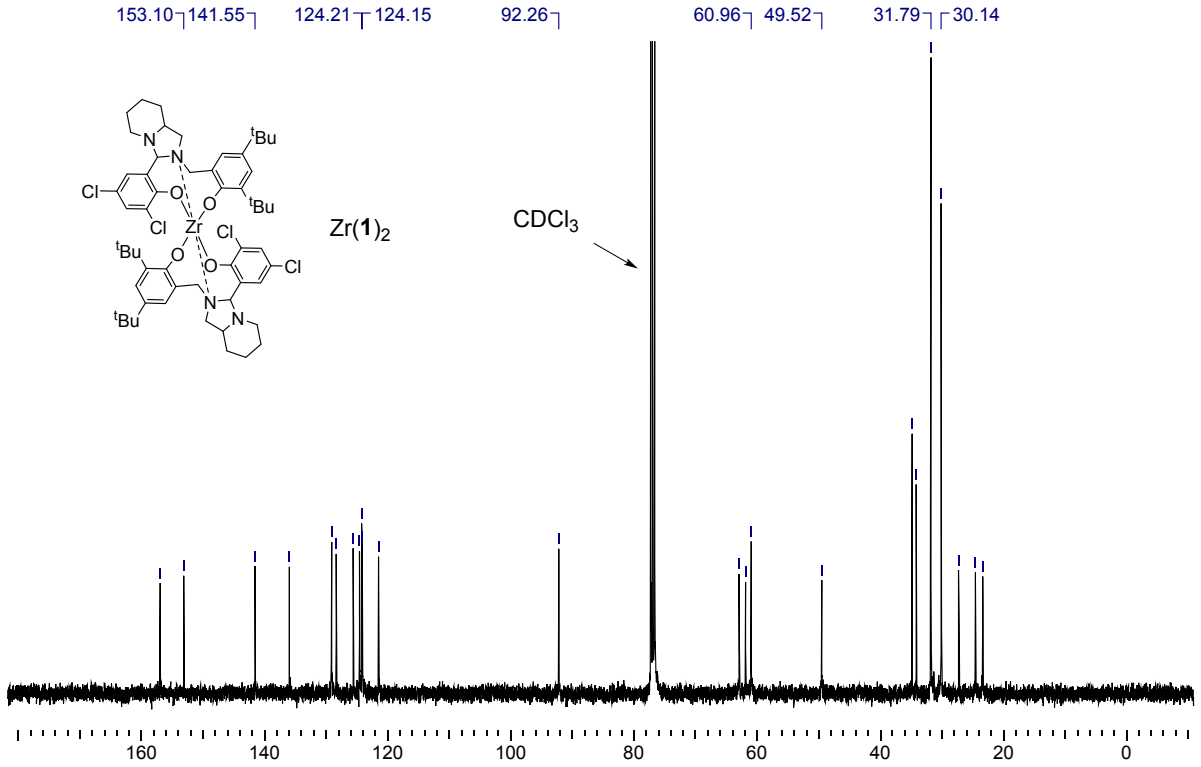

Figure SI12: $^{13}C\{^{1}H\}$ NMR ($CDCl_3$, 100MHz) spectrum of Zr(**1**)$_2$

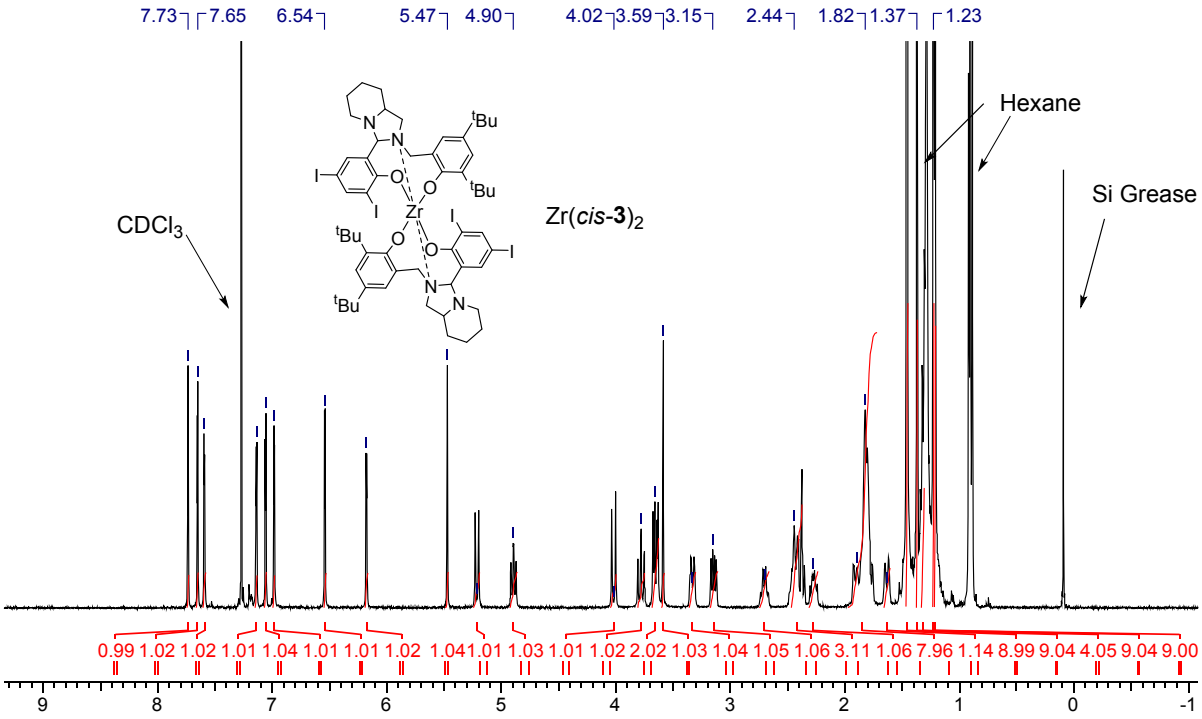

Figure SI13: ^{1}H NMR ($CDCl_3$, 400MHz) spectrum of Zr(*cis*-**3**)$_2$.

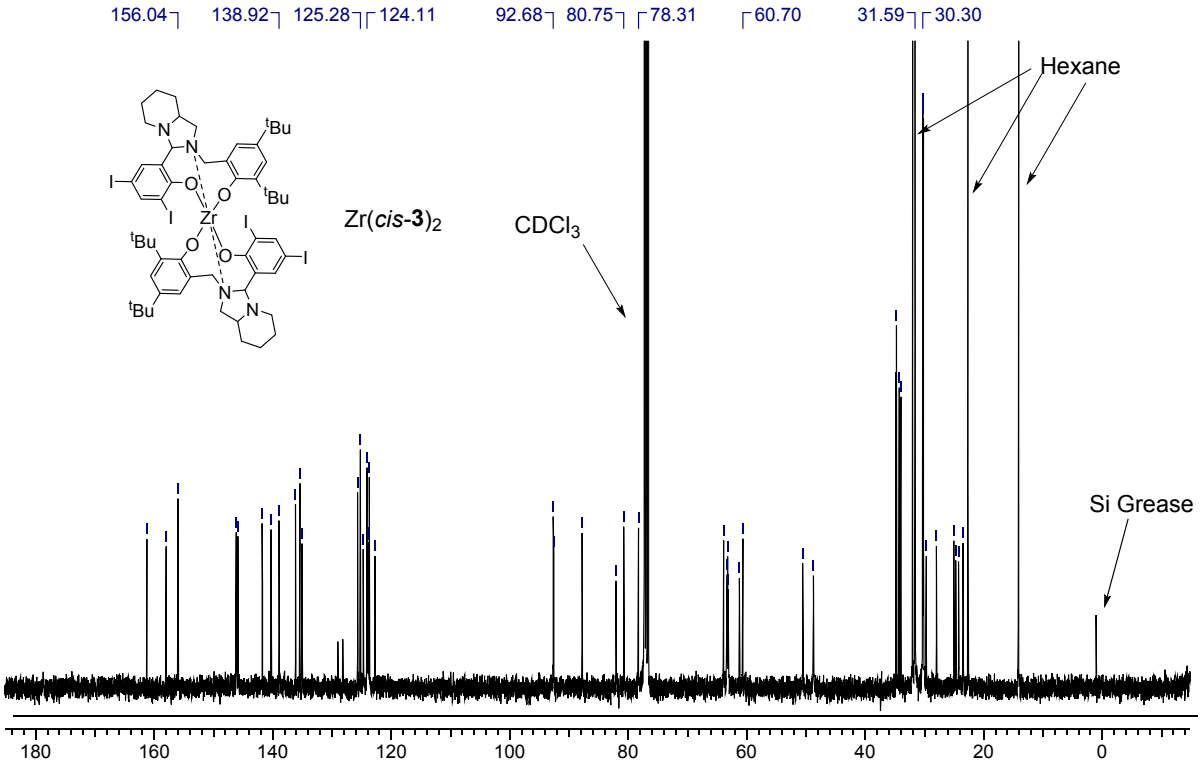

Figure SI14: ^{13}C{^{1}H} NMR ($CDCl_3$, 100MHz) spectrum of Zr(*cis*-**3**)$_2$.

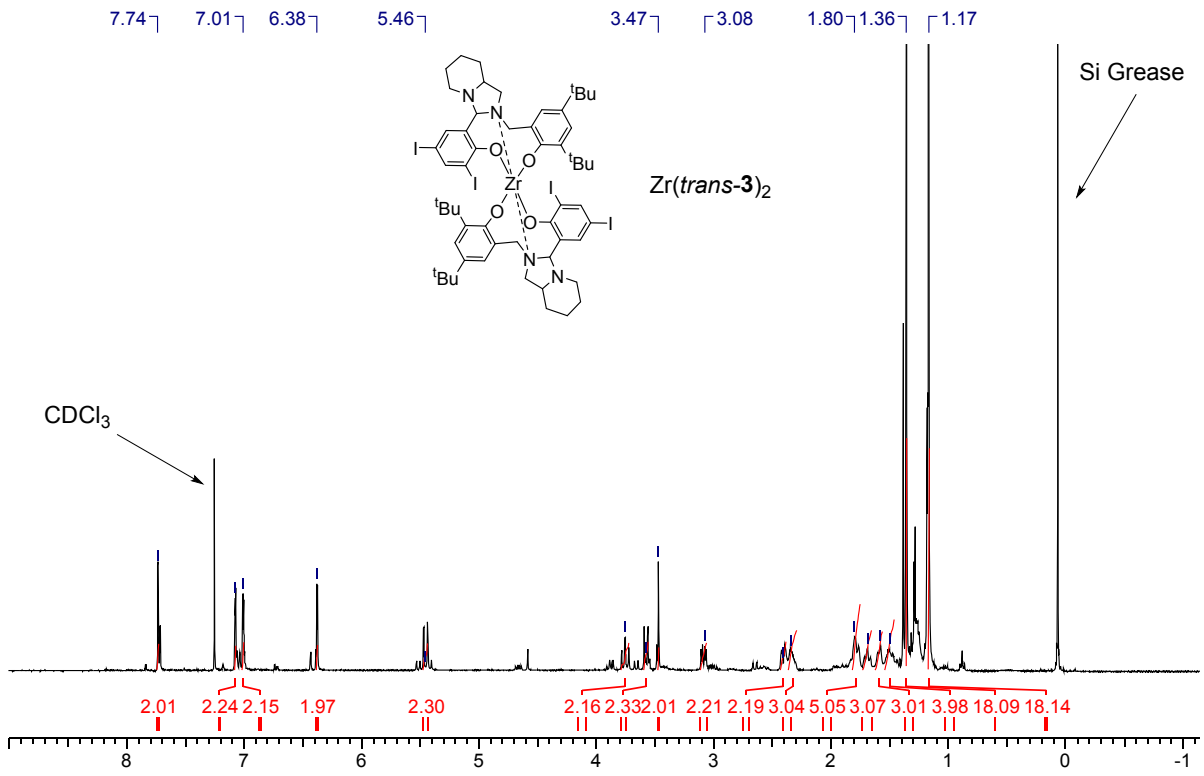

Figure SI15: ^{1}H NMR ($CDCl_3$, 400MHz) spectrum of Zr(*trans*-**3**)$_2$. Note: impurity of another unsymmetrical Zr(**3**)$_2$ isomer.

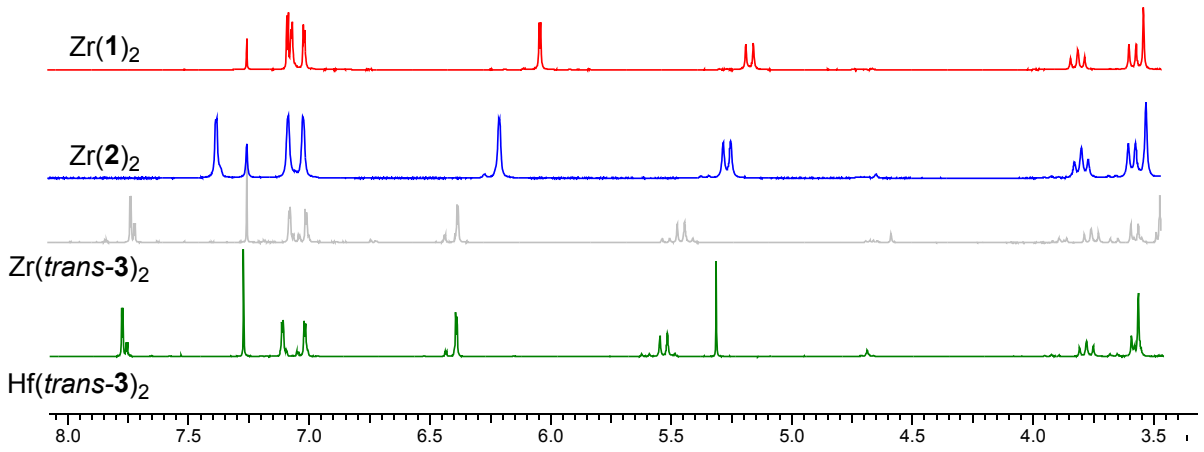

Figure SI16: ^{1}H NMR ($CDCl_3$, 400MHz) spectra comparing Zr(**1-3**)$_2$ and Hf(*trans*-**3**)$_2$.

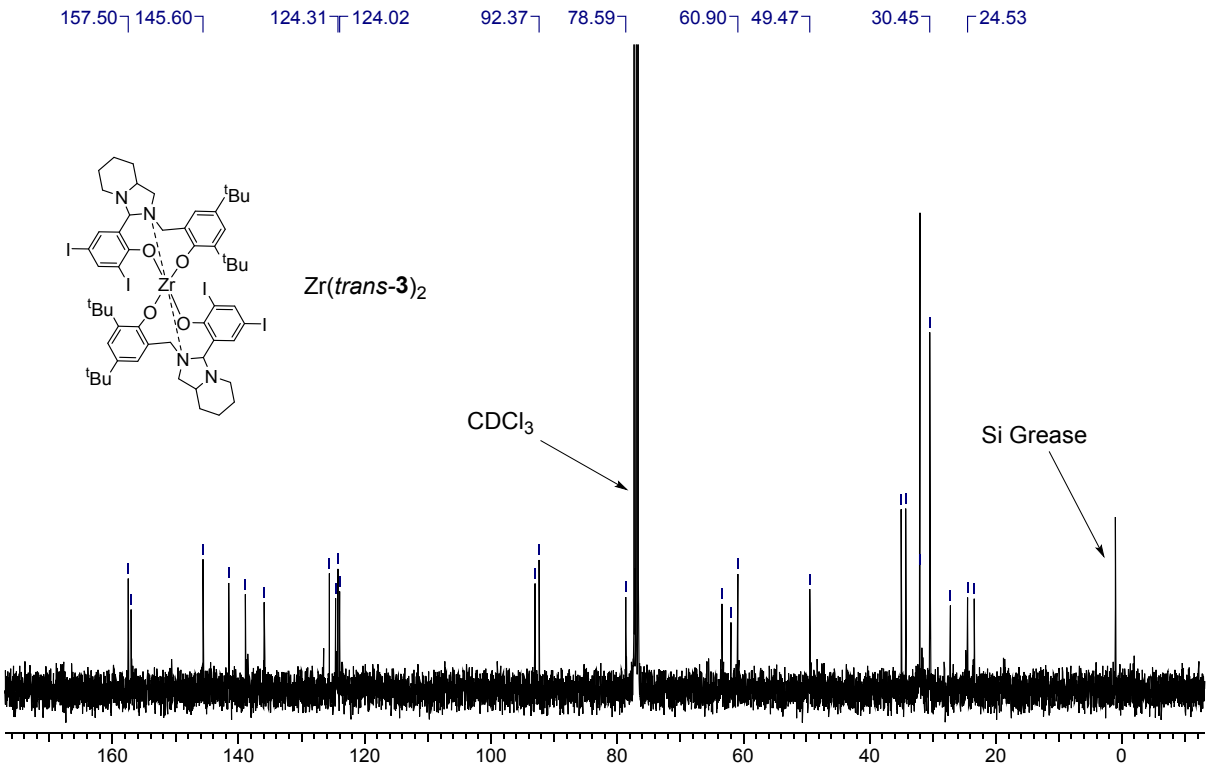

Figure SI17: $^{13}C\{^{1}H\}$ NMR ($CDCl_3$, 100MHz) spectrum of Zr(*trans*-**3**)$_2$.

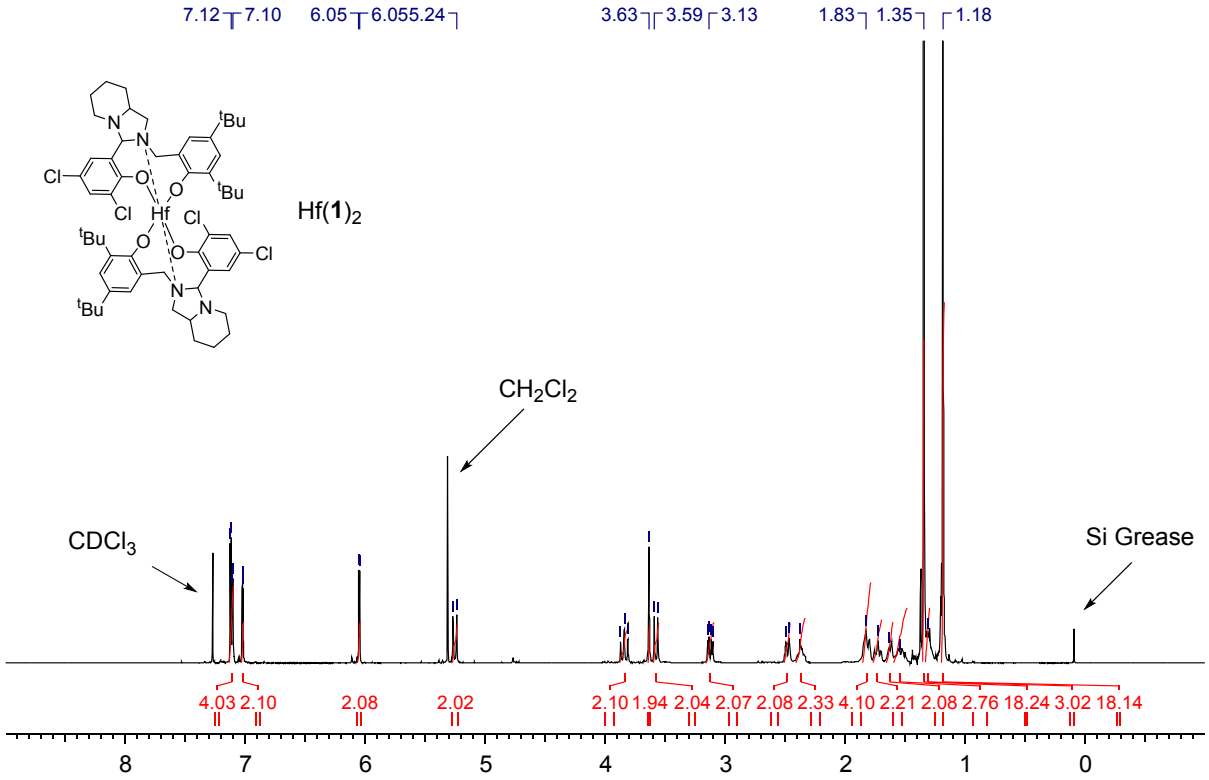

Figure SI18: ^{1}H NMR ($CDCl_3$, 400MHz) spectrum of Hf(**1**)$_2$

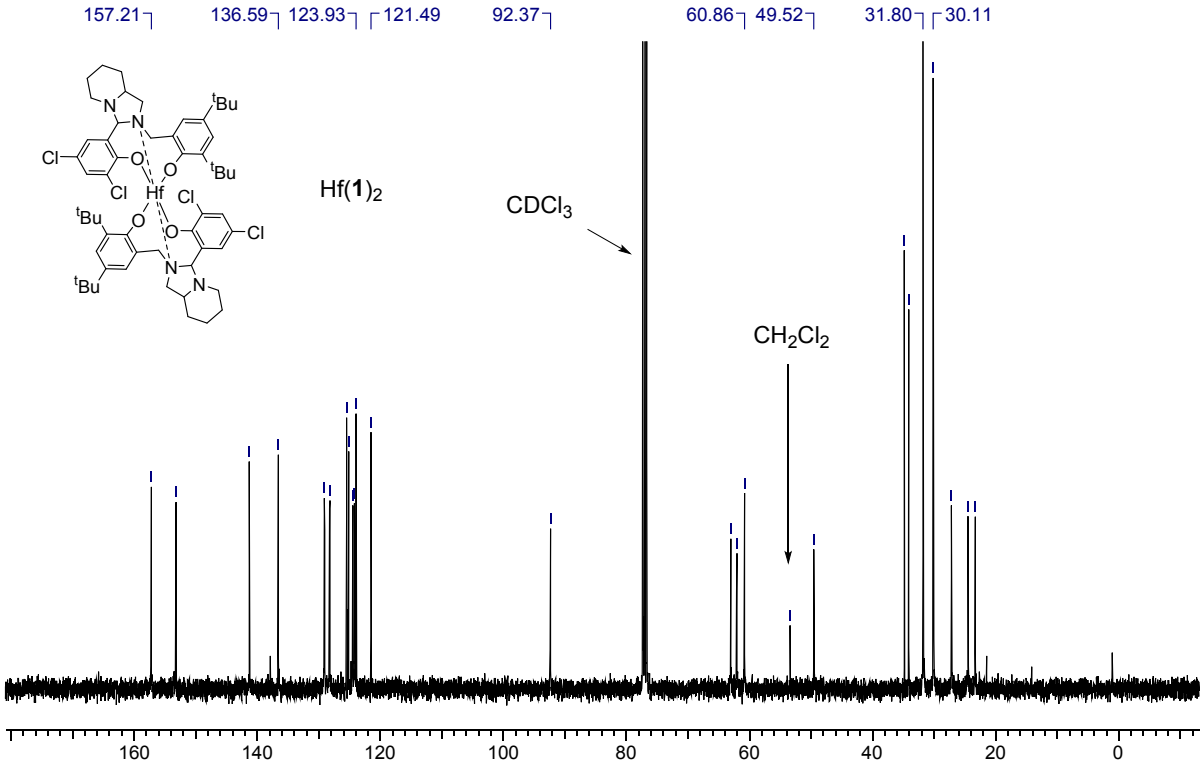

Figure SI19: $^{13}C\{^{1}H\}$ NMR ($CDCl_3$, 100MHz) spectrum of Hf(**1**)$_2$

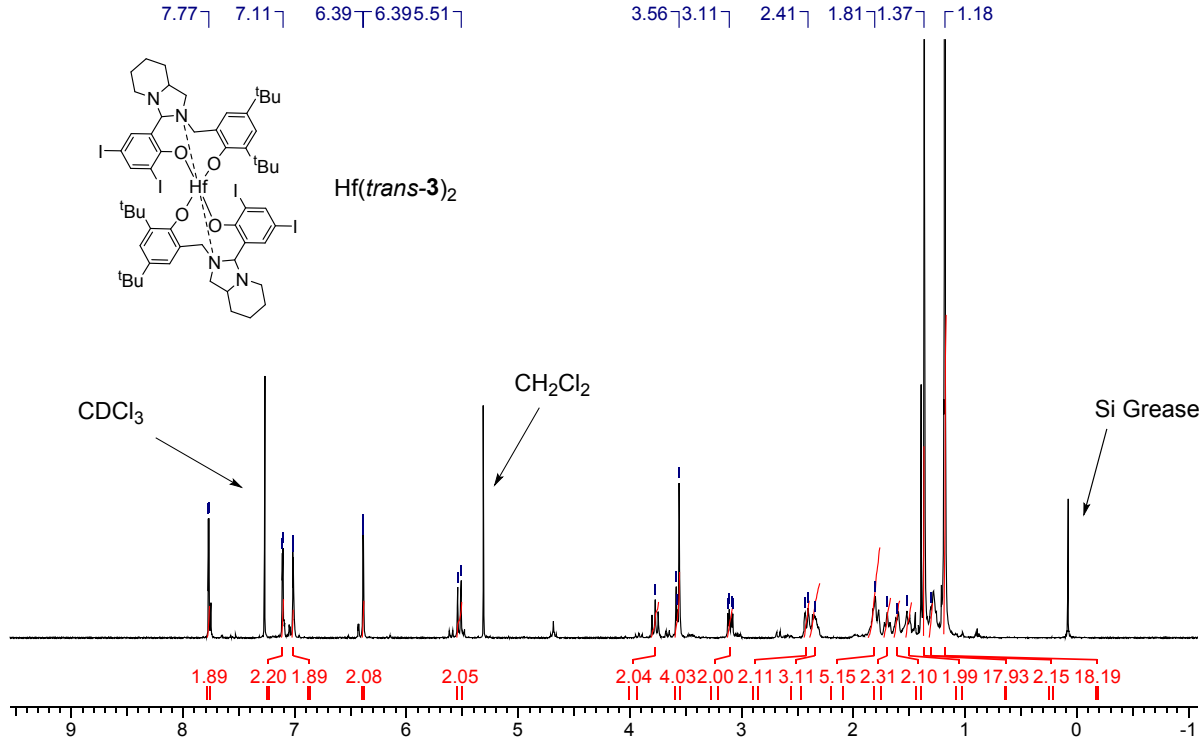

Figure SI20: ^{1}H NMR ($CDCl_3$, 400MHz) spectrum of Hf(*trans*-**3**)$_2$. Note: Impurity of another unsymmetrical Hf(**3**)$_2$ isomer.

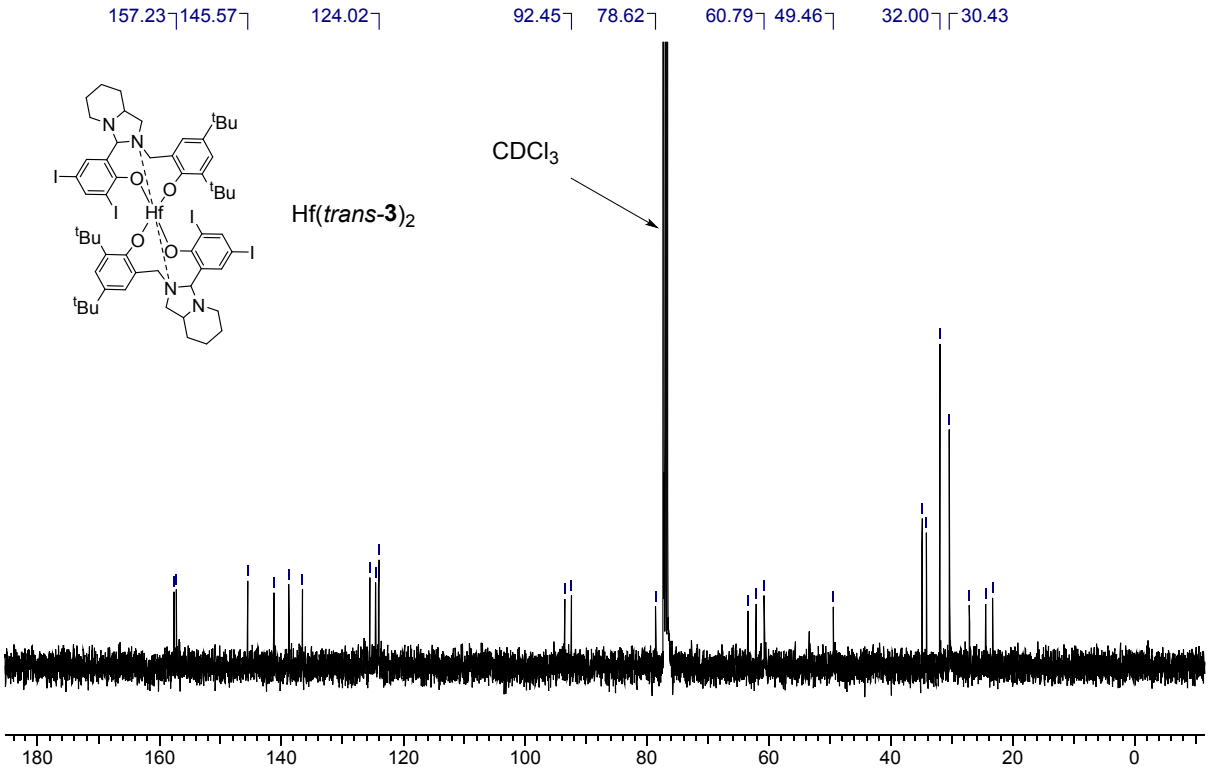

Figure SI21: $^{13}C\{^{1}H\}$ NMR ($CDCl_3$, 100MHz) spectrum of Hf(*trans*-**3**)$_2$.

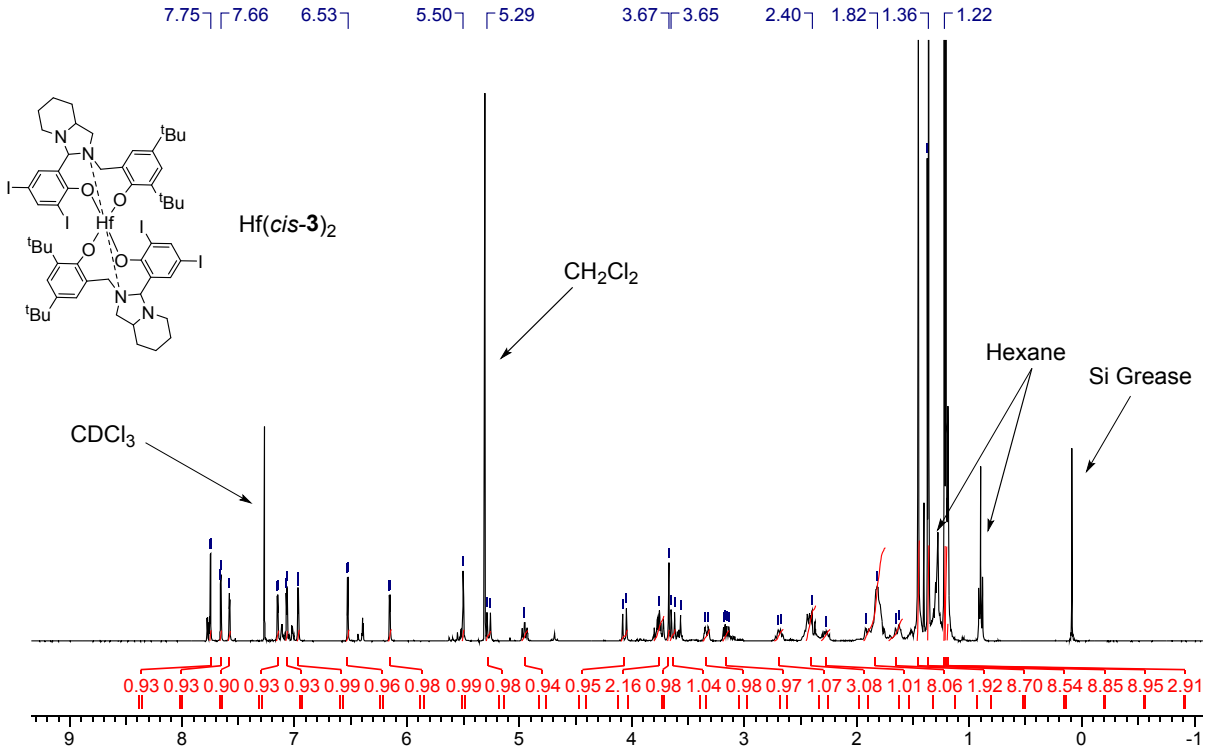

Figure SI22: ^{1}H NMR ($CDCl_3$, 400MHz) spectrum of Hf(*cis*-**3**)$_2$. Note: Impurity of Hf(*trans*-**3**)$_2$ and another unsymmetrical Hf(**3**)$_2$ isomer.

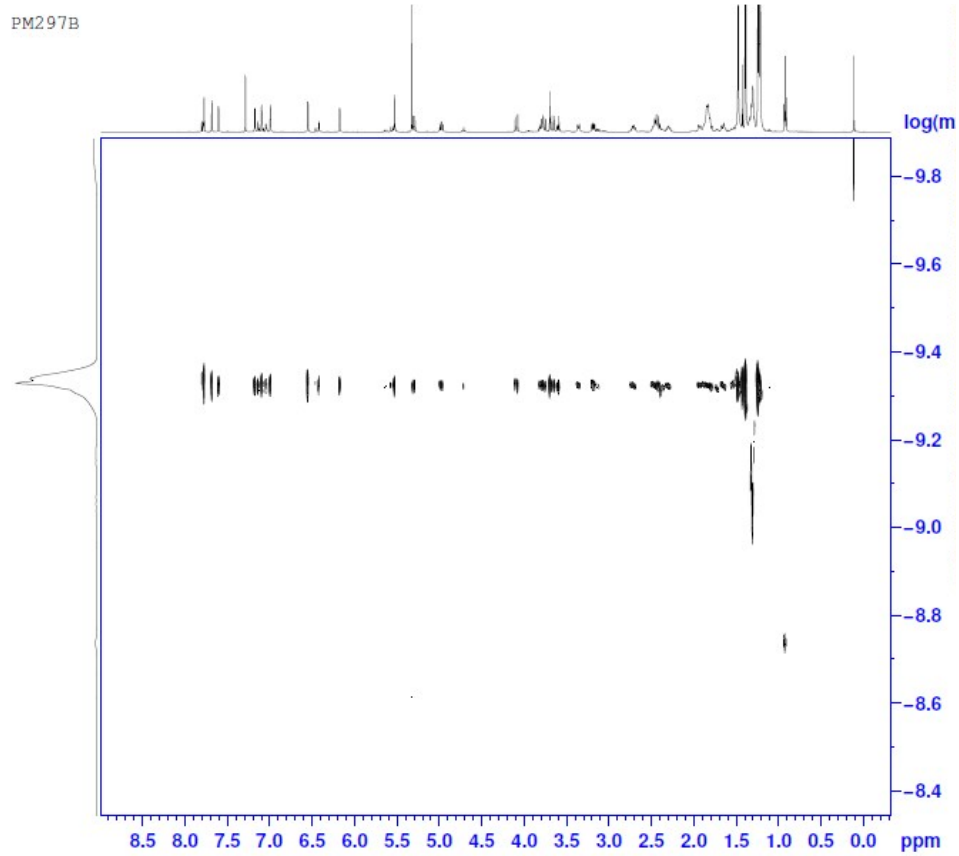

Figure SI23: DOSY NMR ($CDCl_3$, 500MHz) spectrum of Hf(*cis*-**3**)$_2$. Major series (Hf(*cis*-**3**)$_2$) diffusion coefficient = 4.90×10^{-10} m^2 s^{-1}, minor series (Hf(*trans*-**3**)$_2$) diffusion coefficient = 4.78×10^{-10} m^2 s^{-1}.

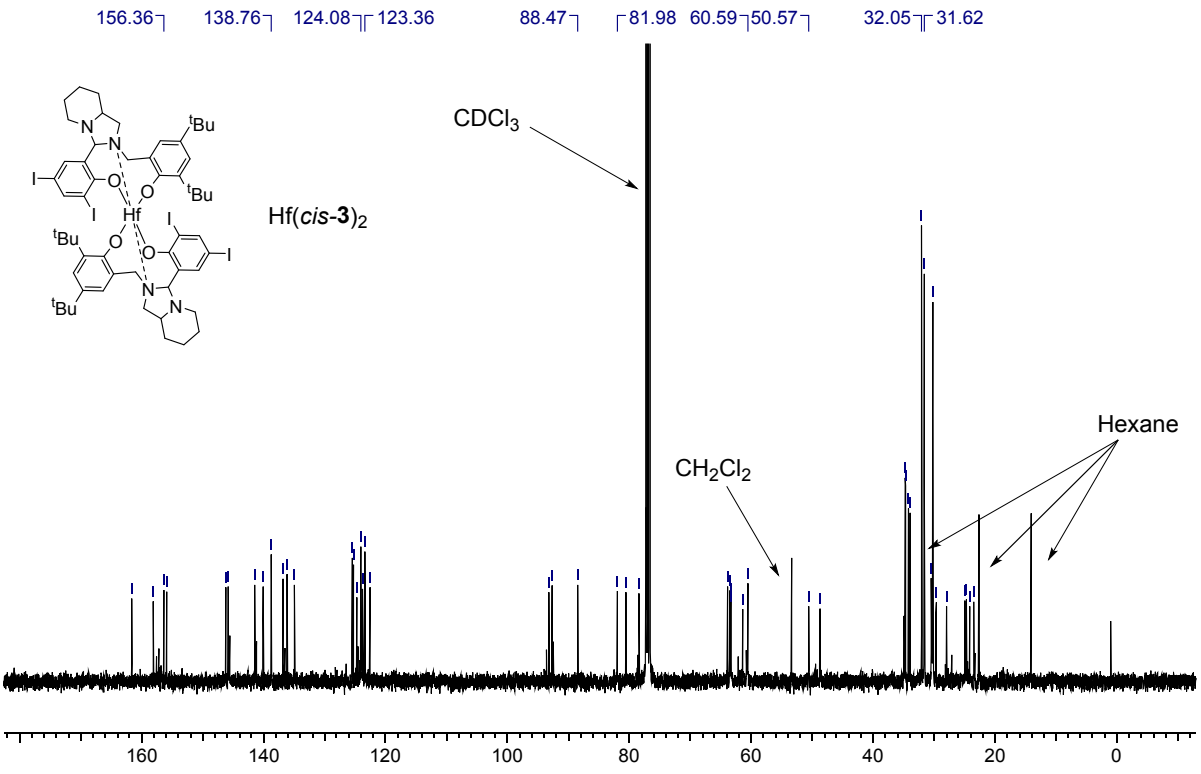

Figure SI24: $^{13}C\{^{1}H\}$ NMR ($CDCl_3$, 100MHz) spectrum of Hf(*cis*-**3**)$_2$.

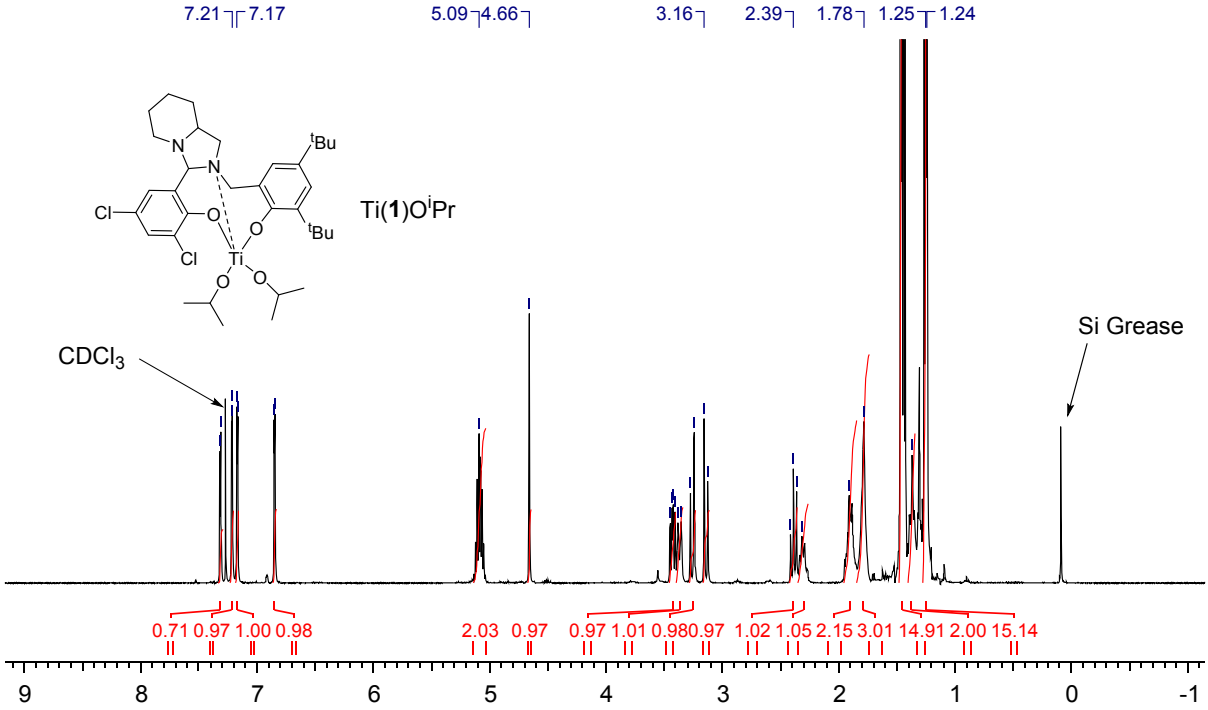

Figure SI25: ^{1}H NMR ($CDCl_3$, 400MHz) spectrum of Ti(**1**)(O^iPr)$_2$

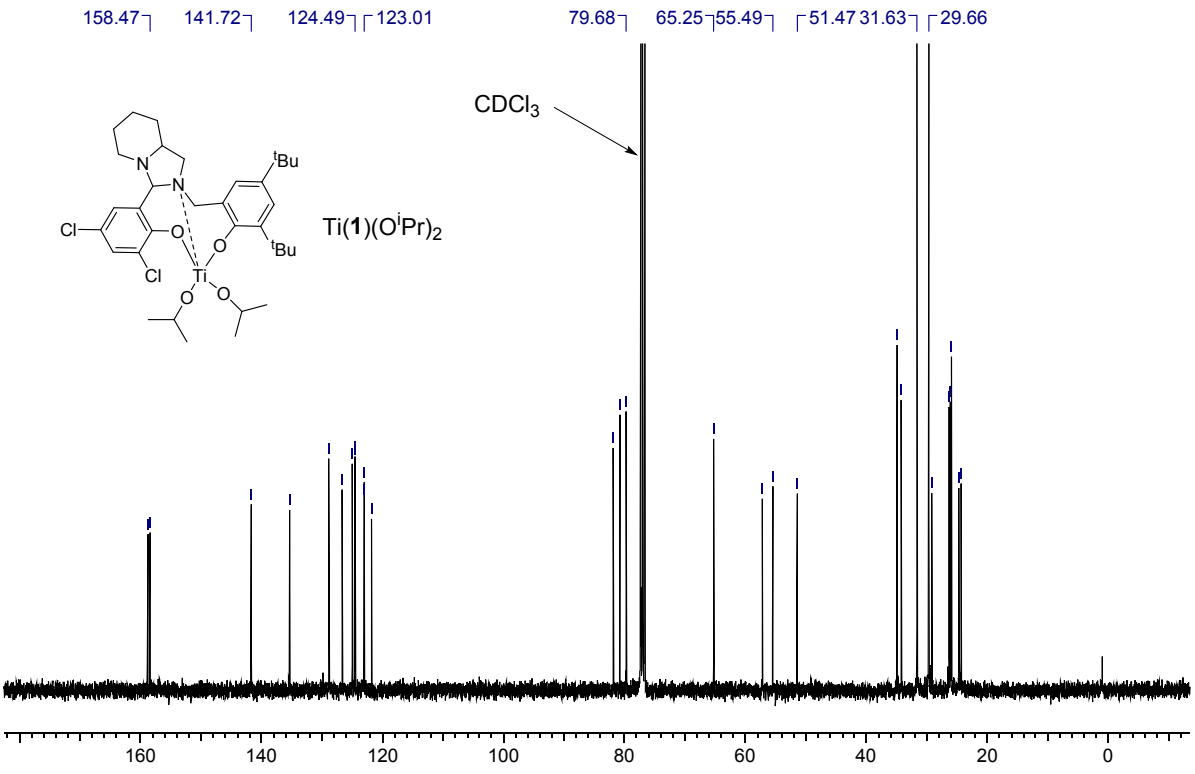

Figure SI26: $^{13}C\{^{1}H\}$ NMR ($CDCl_3$, 100MHz) spectrum of Ti(**1**)(O^iPr)$_2$

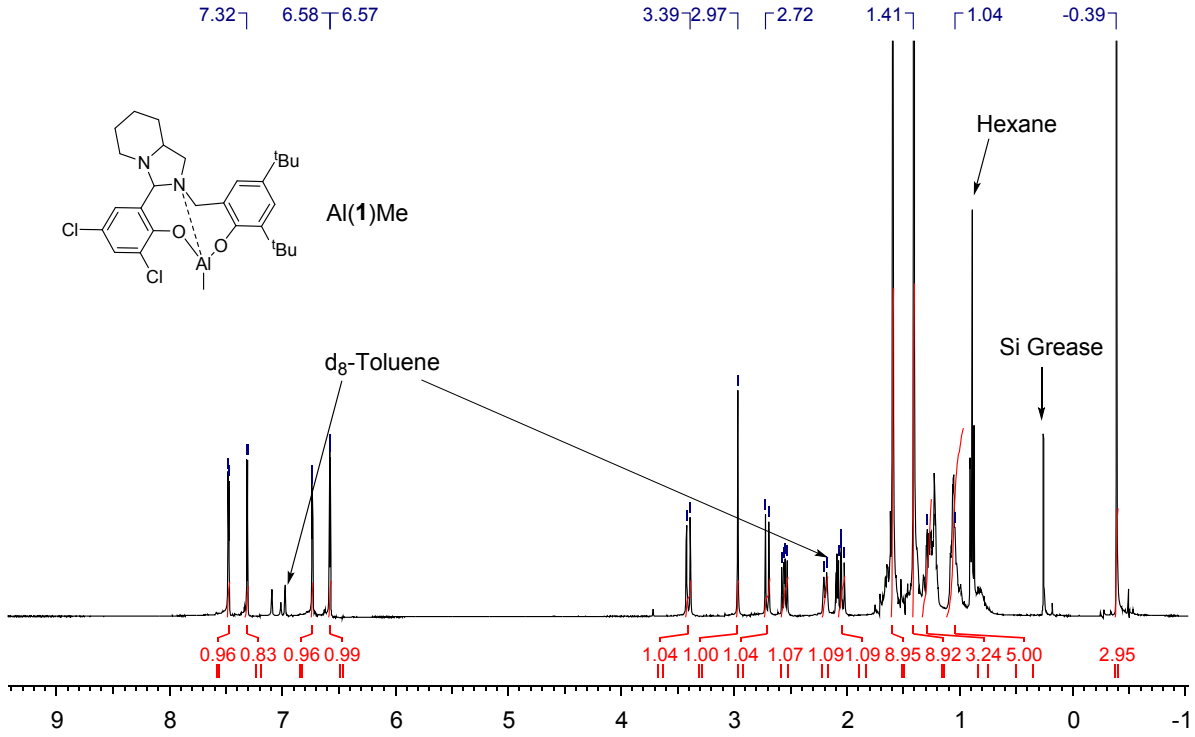

Figure SI27: ^{1}H NMR (d_8-toluene, 400MHz) spectrum of Al(**1**)Me

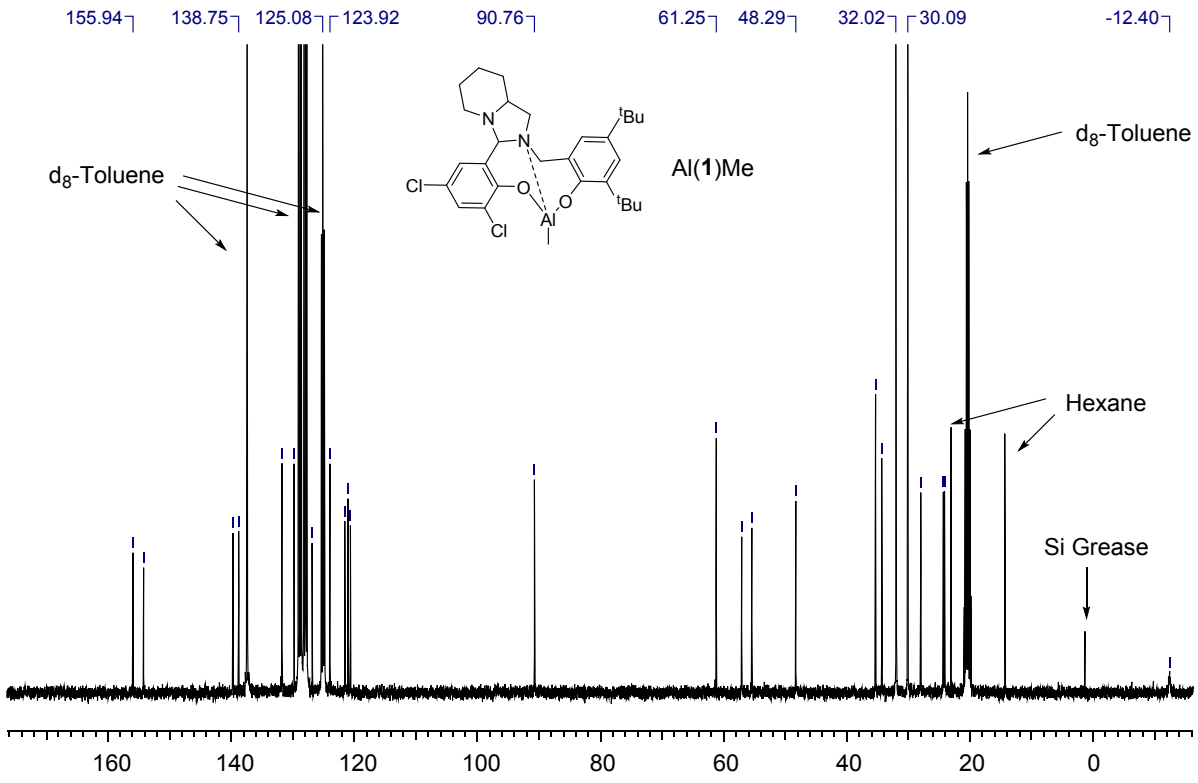

Figure SI28: $^{13}C\{^{1}H\}$ NMR (d_8-toluene, 100MHz) spectrum Al(**1**)Me

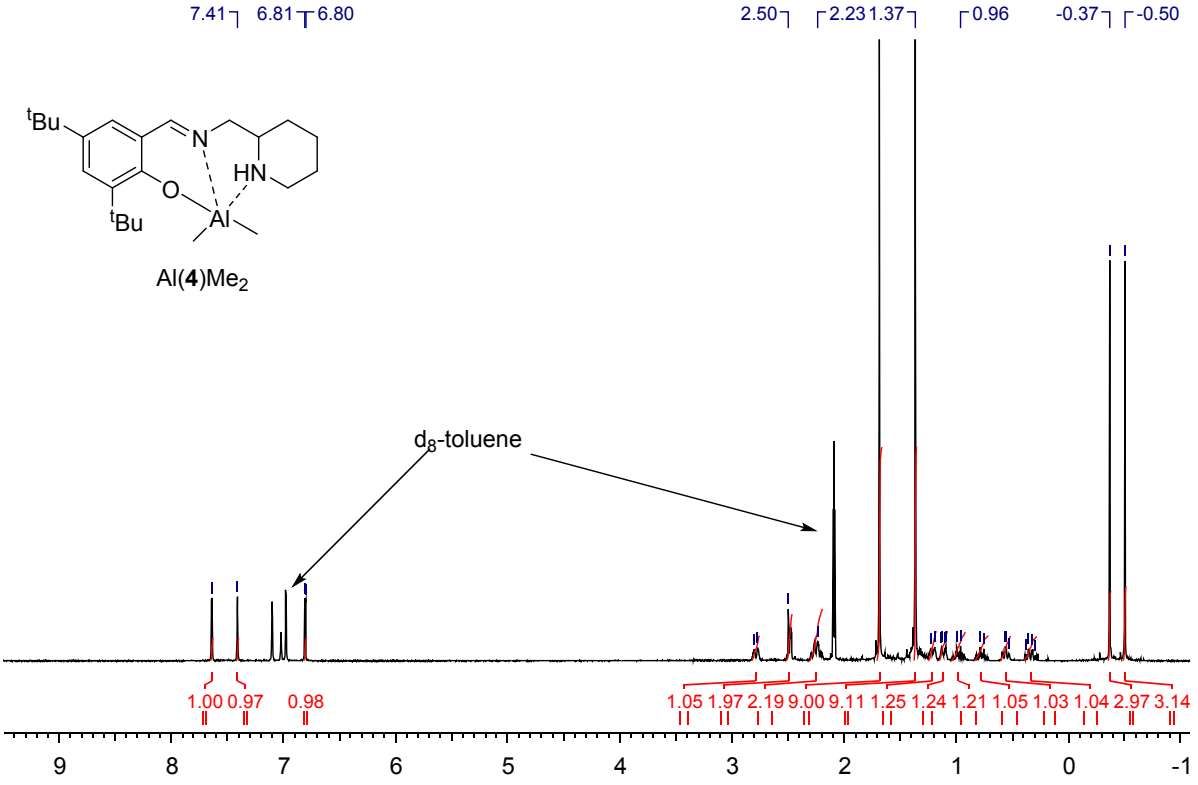

Figure SI29: ^{1}H NMR (d_8-toluene, 400MHz) spectrum of Al(**4**)Me_2

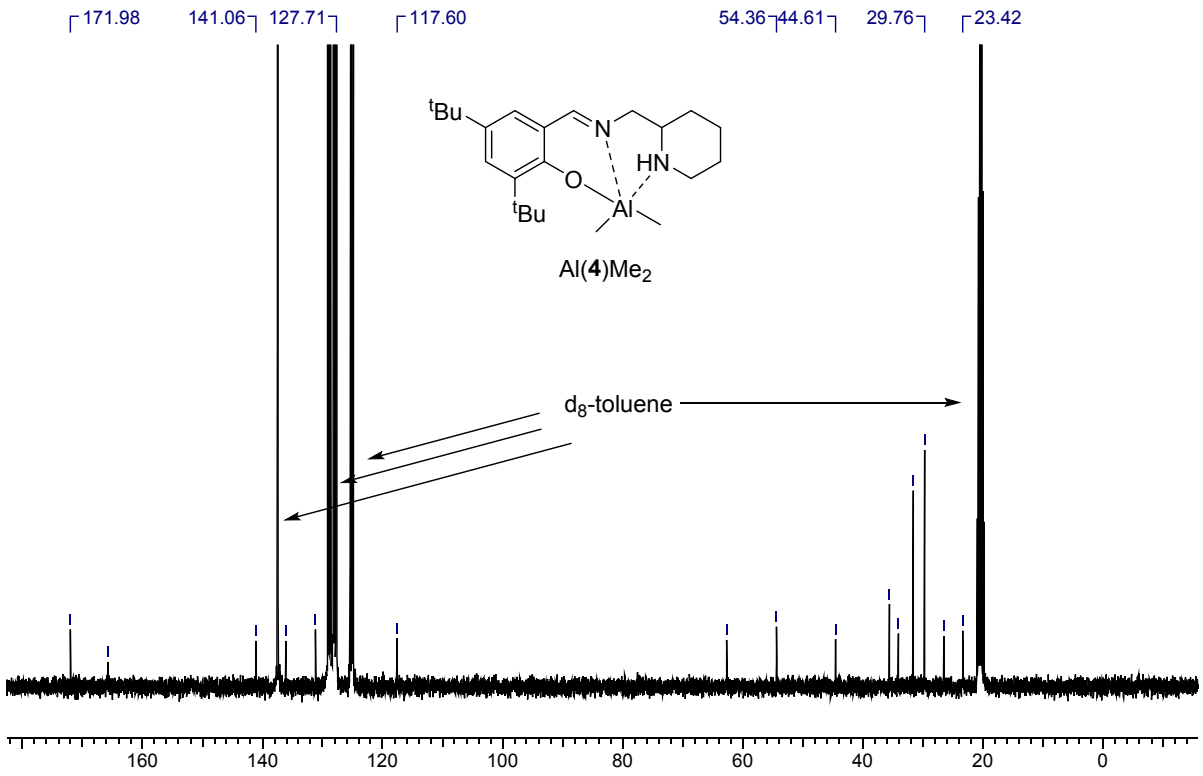

Figure SI30: $^{13}C\{^{1}H\}$ NMR (d_8-toluene, 100MHz) spectrum Al(**4**)Me_2

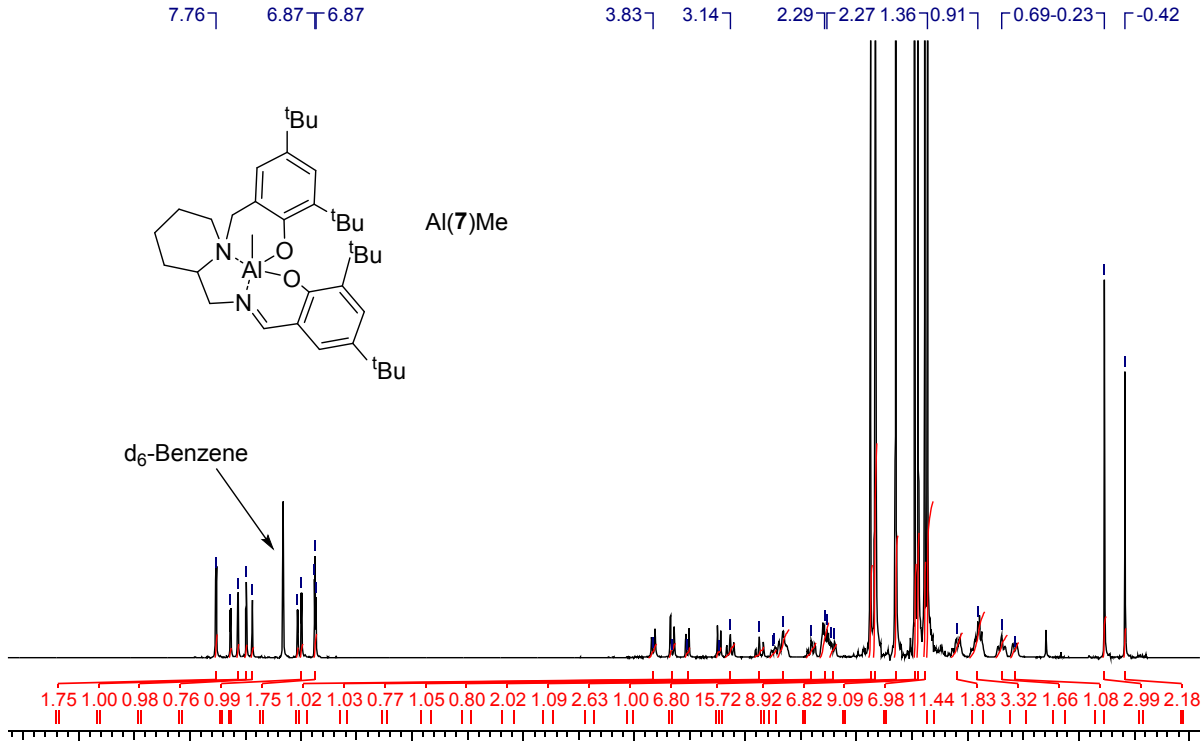

Figure SI31: ^{1}H NMR (d_6-benzene, 400MHz) spectrum of Al(**7**)Me.

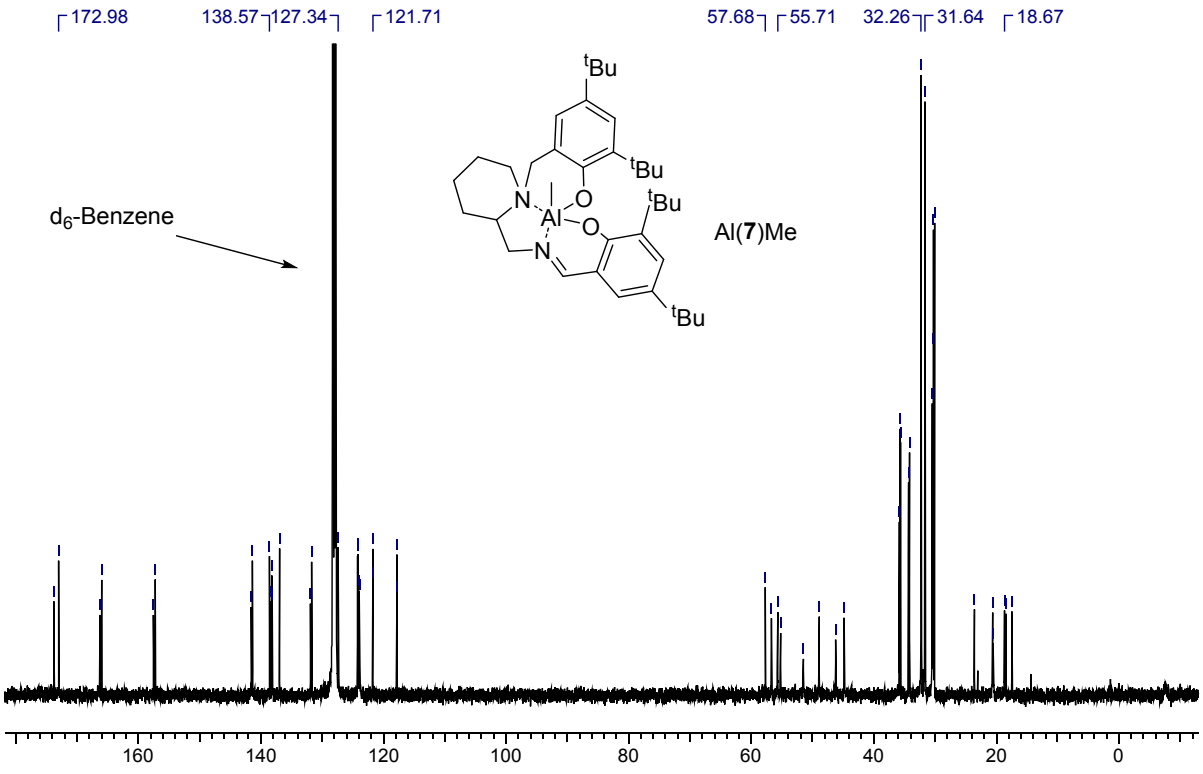

Figure SI32: $^{13}C\{^{1}H\}$ NMR (d_6-benzene, 100MHz) spectrum Al(**7**)Me

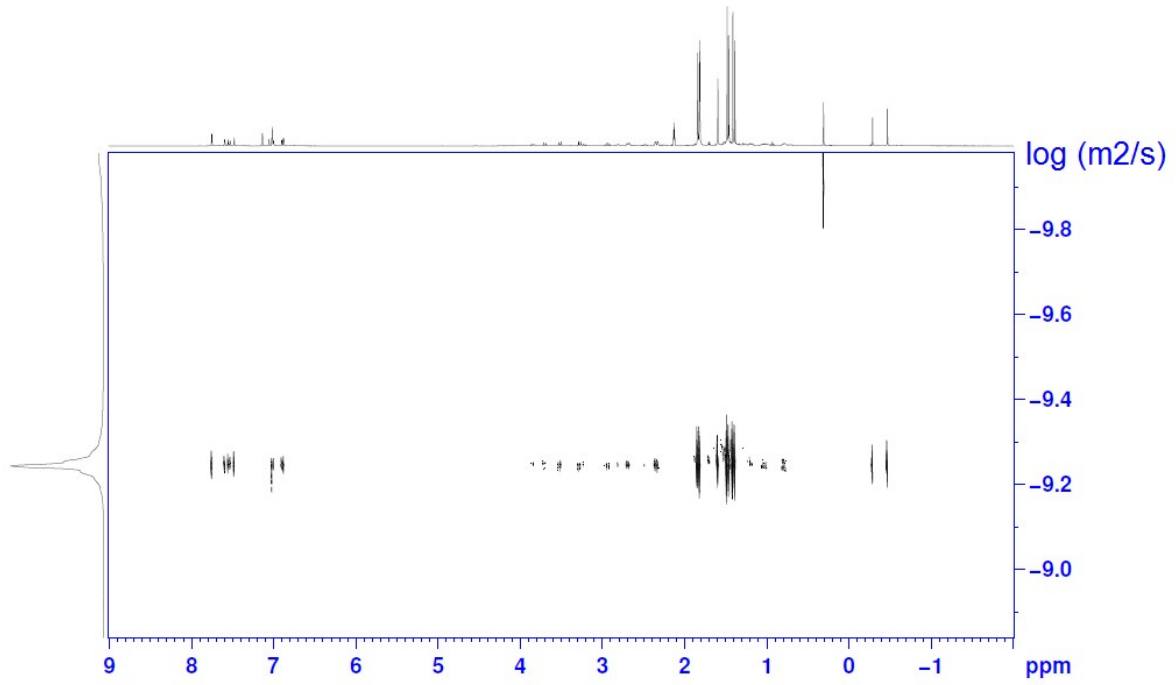

Figure SI33: DOSY NMR (d_8-toluene, 500MHz) spectrum of Al(**7**)Me

Selected Polymer Characterisation

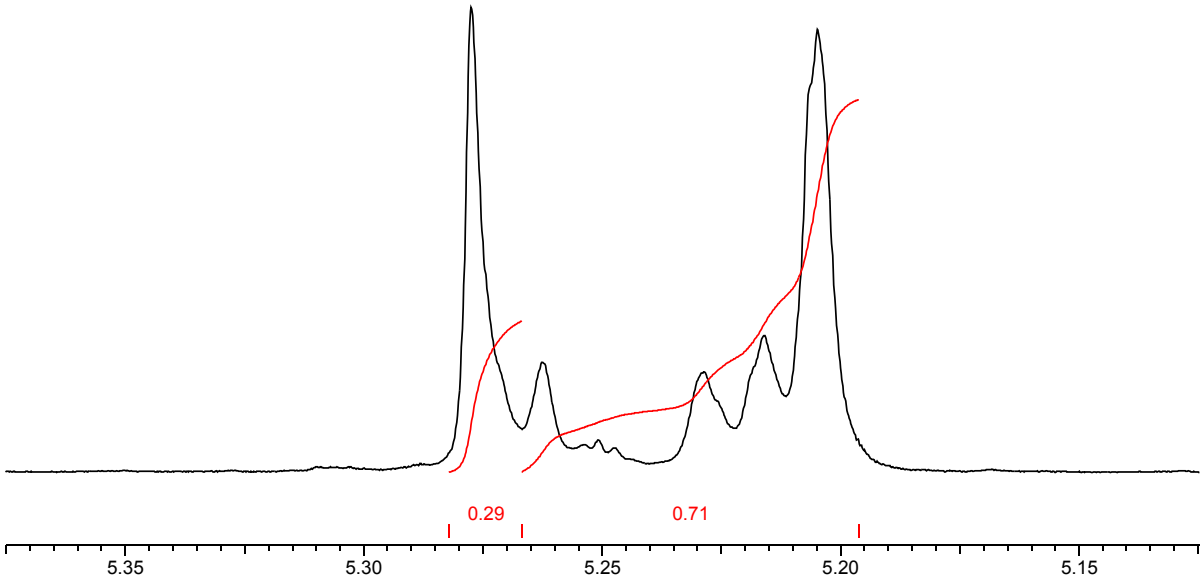

Figure SI34: ^{1}H NMR ($CDCl_3$, 400MHz) spectrum of heterotactic PLA synthesised from solution polymerisation with Zr(**1**)$_2$ – table 2, entry 1.

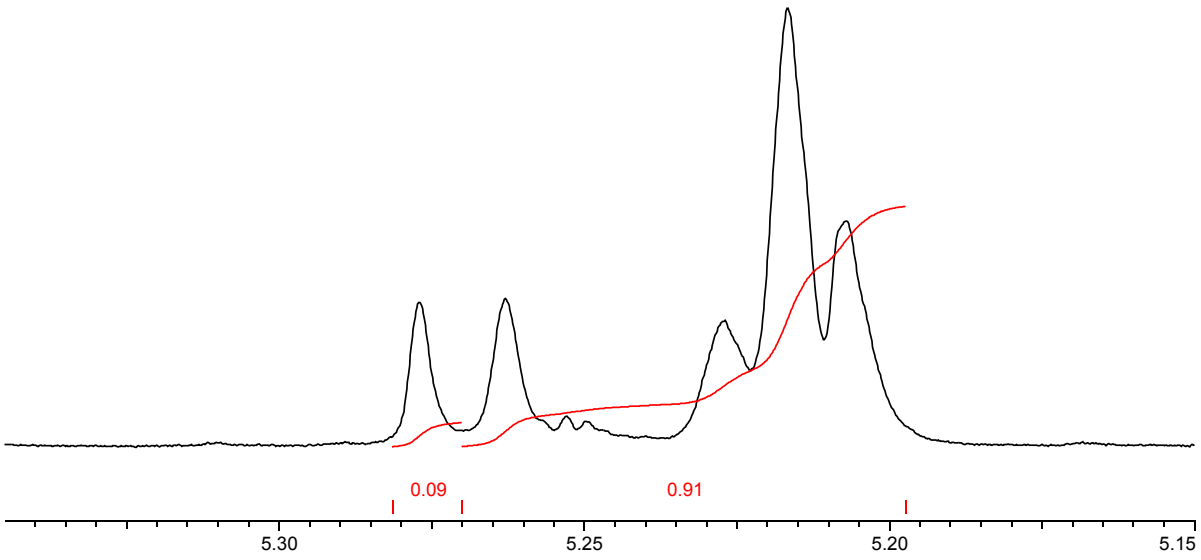

Figure SI35: ^{1}H NMR ($CDCl_3$, 400MHz) spectrum of PLA synthesised from bulk polymerisation with Zr(**1**)$_2$ – table 2, entry 3.

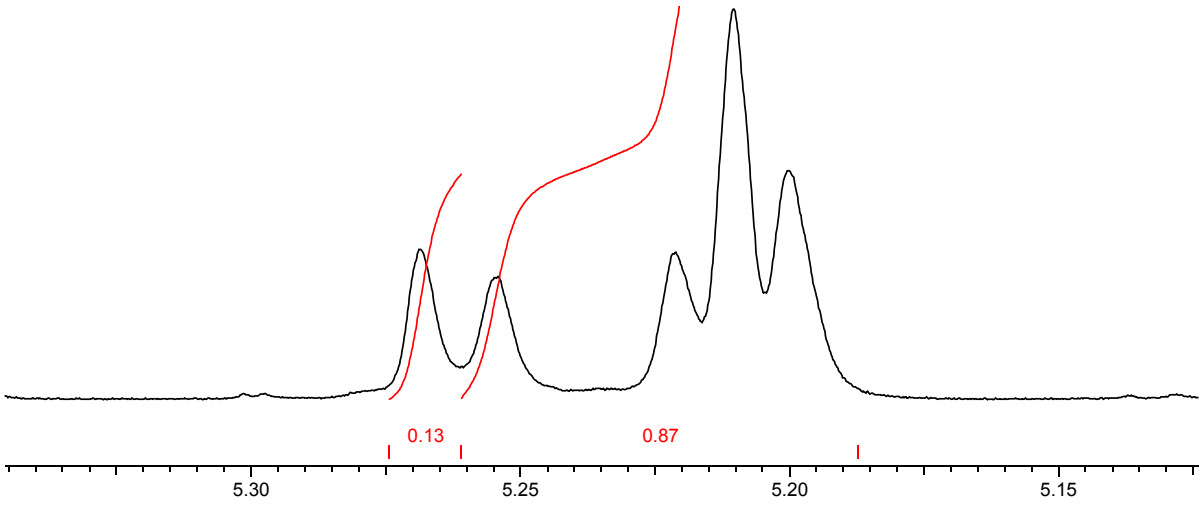

Figure SI36: ^{1}H NMR ($CDCl_3$, 400MHz) spectrum of atactic PLA synthesised from bulk polymerisation with Ti(**1**)($O^{i}Pr$)$_2$ – table 2, entry 12.

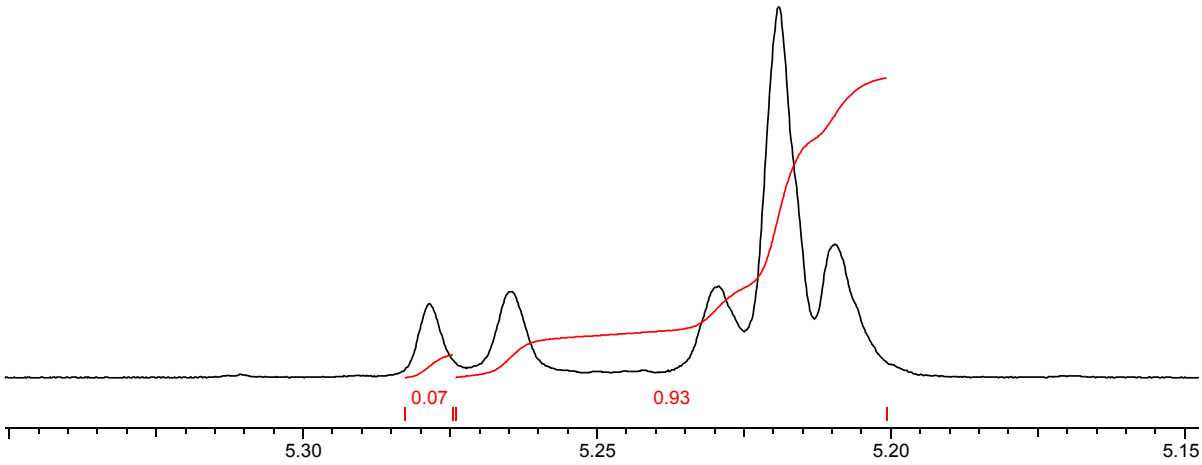

Figure SI37: ^{1}H NMR ($CDCl_3$, 400MHz) spectrum of isotactic PLA synthesised from solution polymerisation with Al(**7**)Me table 3, entry 7.

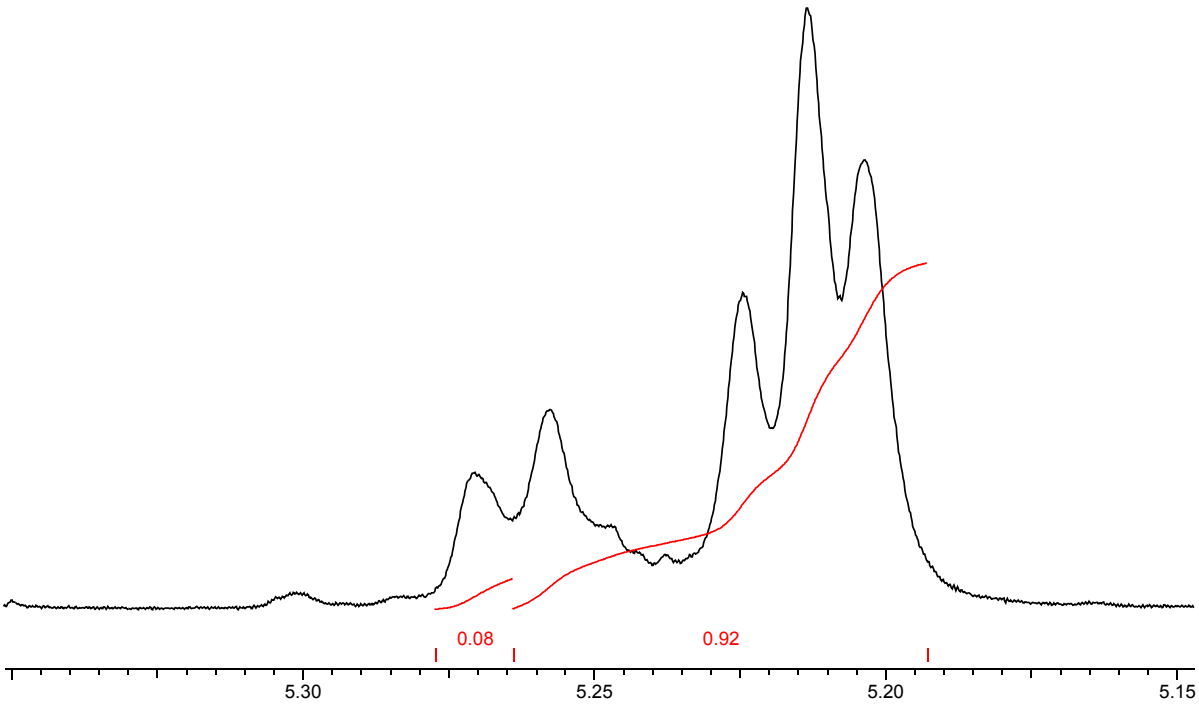

Figure SI38: ^{1}H NMR ($CDCl_3$, 400MHz) spectrum of PLA synthesised from bulk polymerisation with **1**H_2.

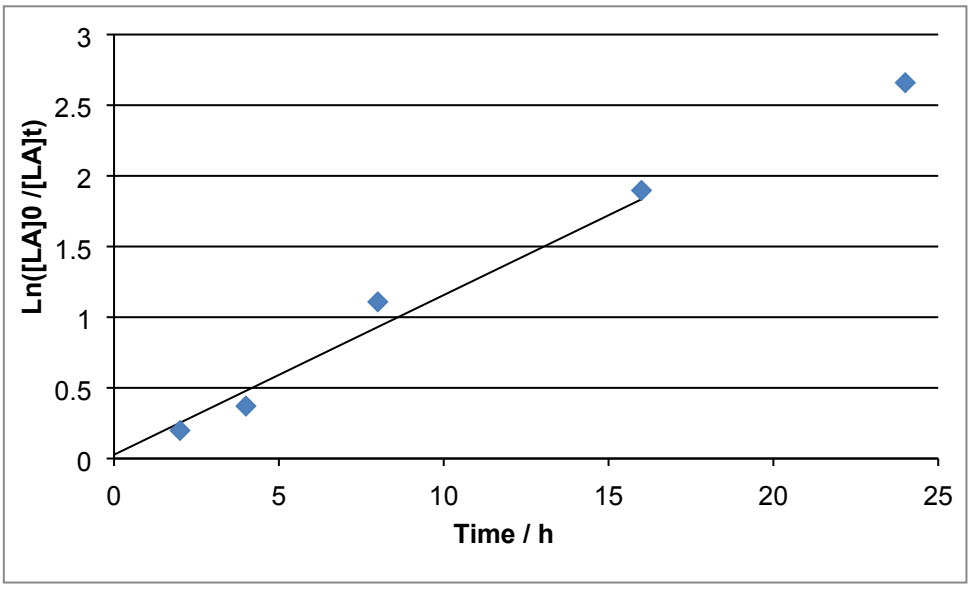

Figure SI39: Semi-logarithmic plot for the solution polymerisation of Zr(**1**)$_2$. Conditions: Toluene, 80°C, [LA]:[Zr(**1**)$_2$]:[BnOH] = 100:1:1

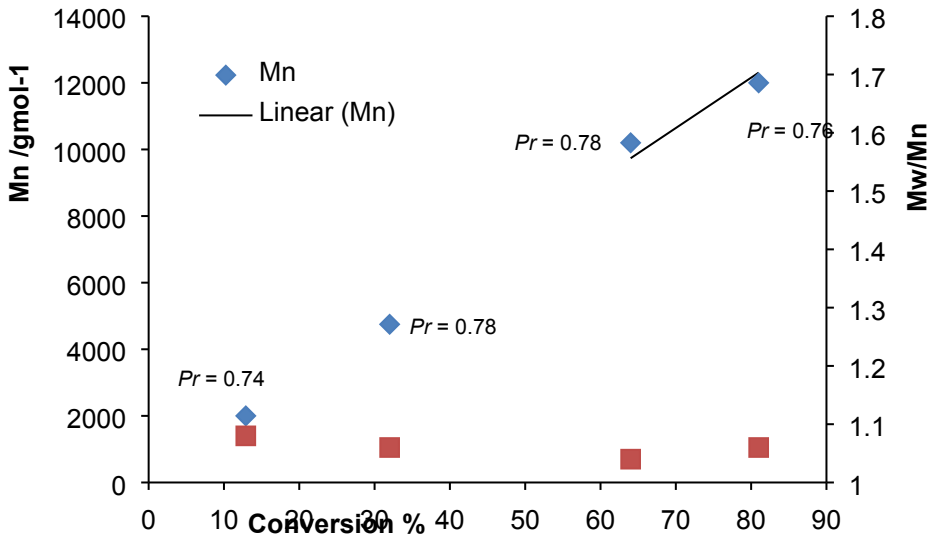

Figure SI40: M_n and M_w/M_n against conversion for solution polymerisation of Zr(**2**)$_2$. Linear regression gave the equation of the line at y = 151× + 59.

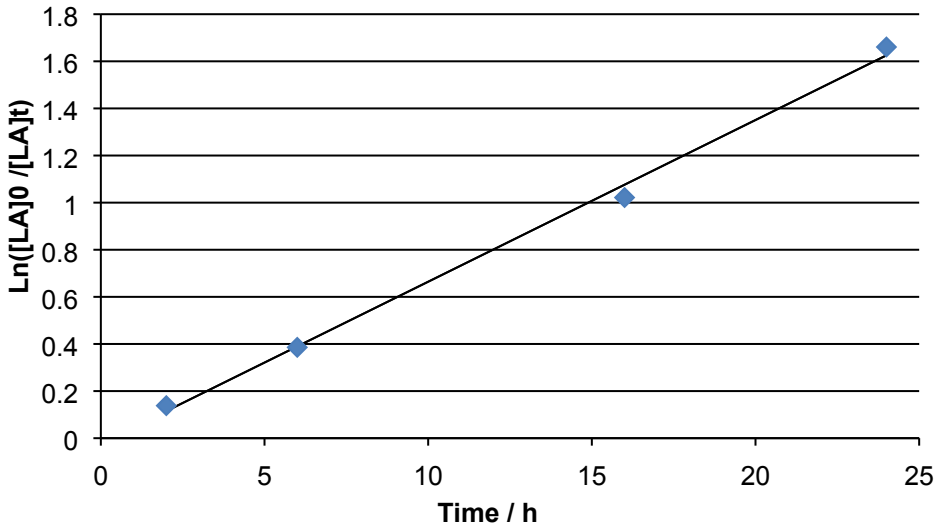

Figure SI41: Semi-logarithmic plot for the solution polymerisation of Zr(**2**)$_2$. Conditions: Toluene, 80°C, [LA]:[Zr(**1**)$_2$]:[BnOH] = 100:1:1

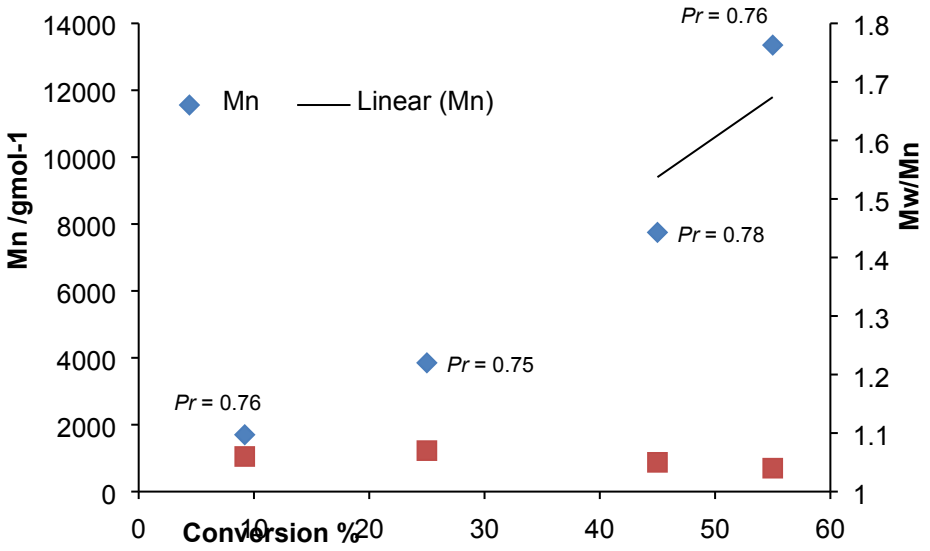

Figure SI42: M_n and M_w/M_n against conversion for solution polymerisation of Hf(**1**)$_2$. Linear regression gave the equation of the line at y = 239× – 1364(R^2 = 0.92)

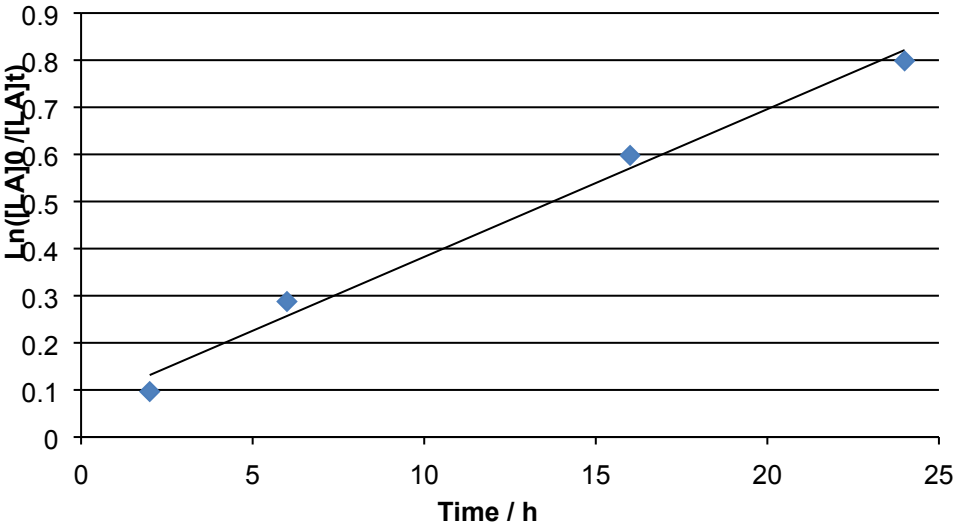

Figure SI43: Semi-logarithmic plot for the solution polymerisation of Hf(**1**)$_2$. Conditions: Toluene, 80°C, [LA]:[Zr(**1**)$_2$]:[BnOH] = 100:1:1

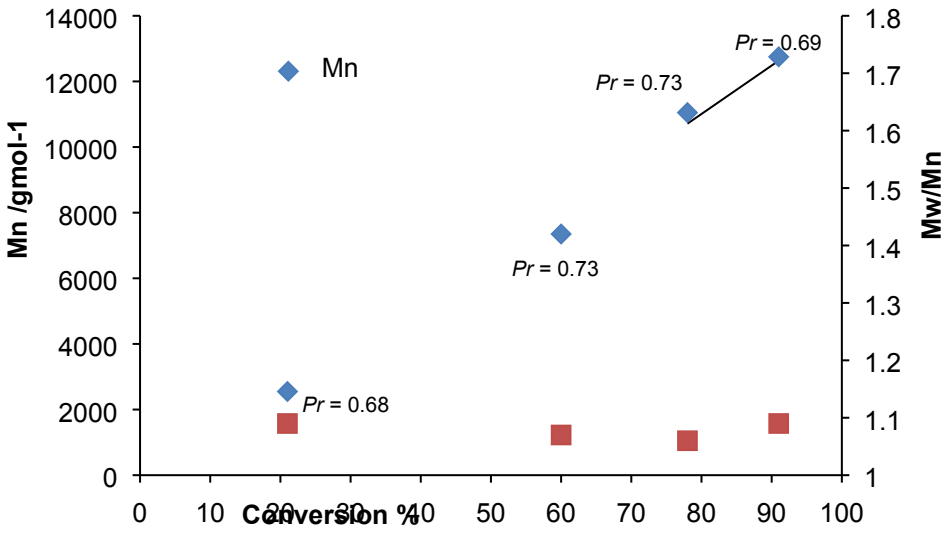

Figure SI44: M_n and M_w/M_n against conversion for solution polymerisation of Al(**4**)Me_2. Linear regression gave the equation of the line at y = 148× – 799(R^2 = 0.99).

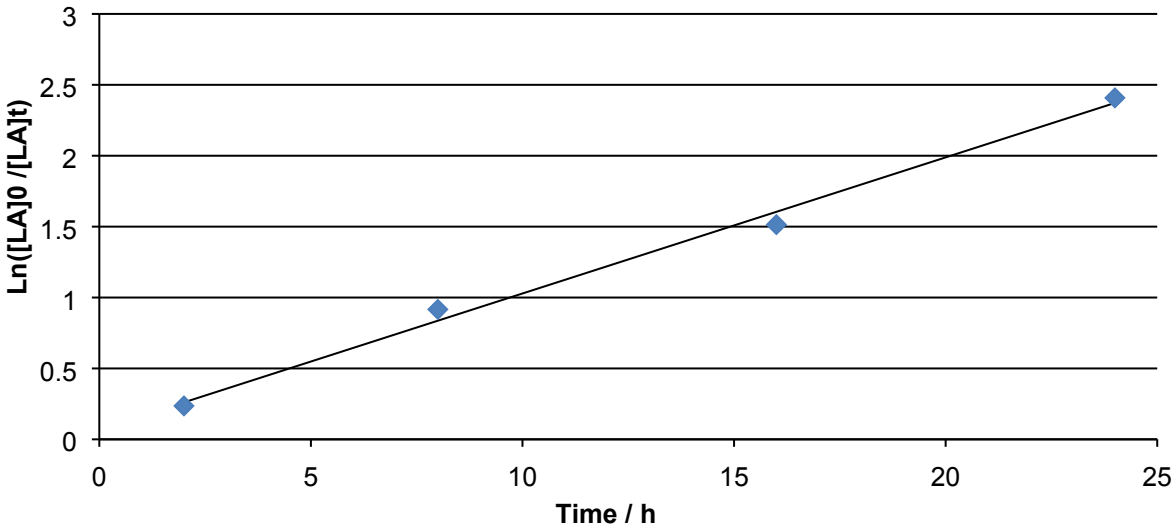

Figure SI45: Semi-logarithmic plot for the solution polymerisation of Al(**4**)Me_2. Conditions: Toluene, 80°C, [LA]:[Zr(**1**)$_2$]:[BnOH] = 100:1:1

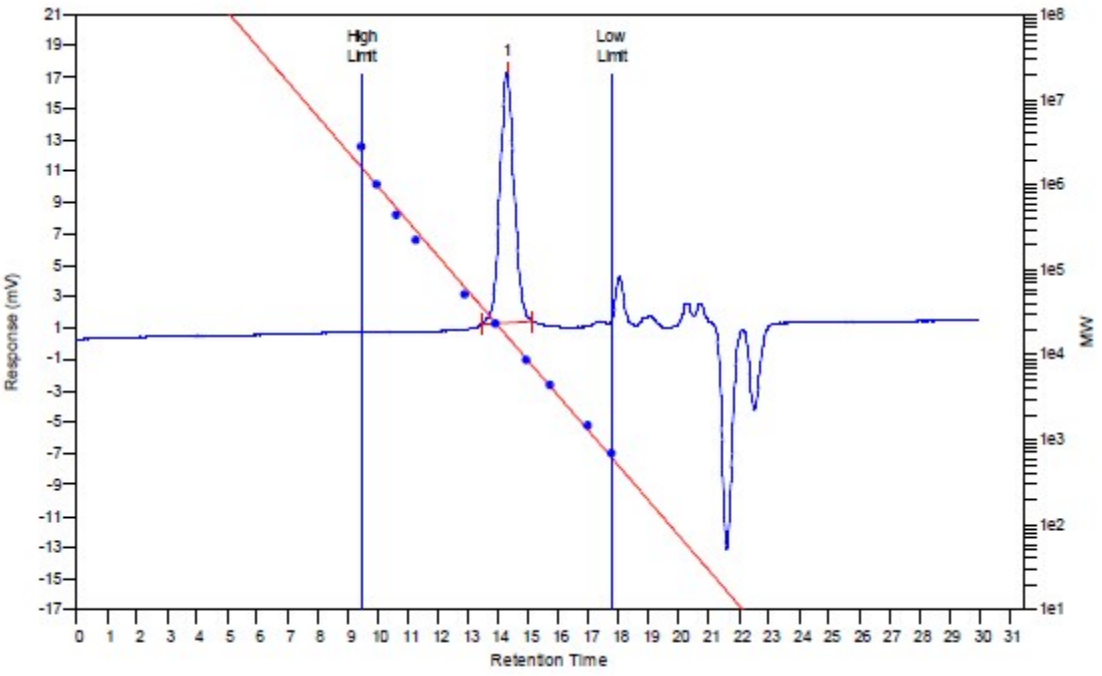

Figure SI46: GPC trace of PLA prepared in solution with Zr(**1**)$_2$ – table 2, entry 1.

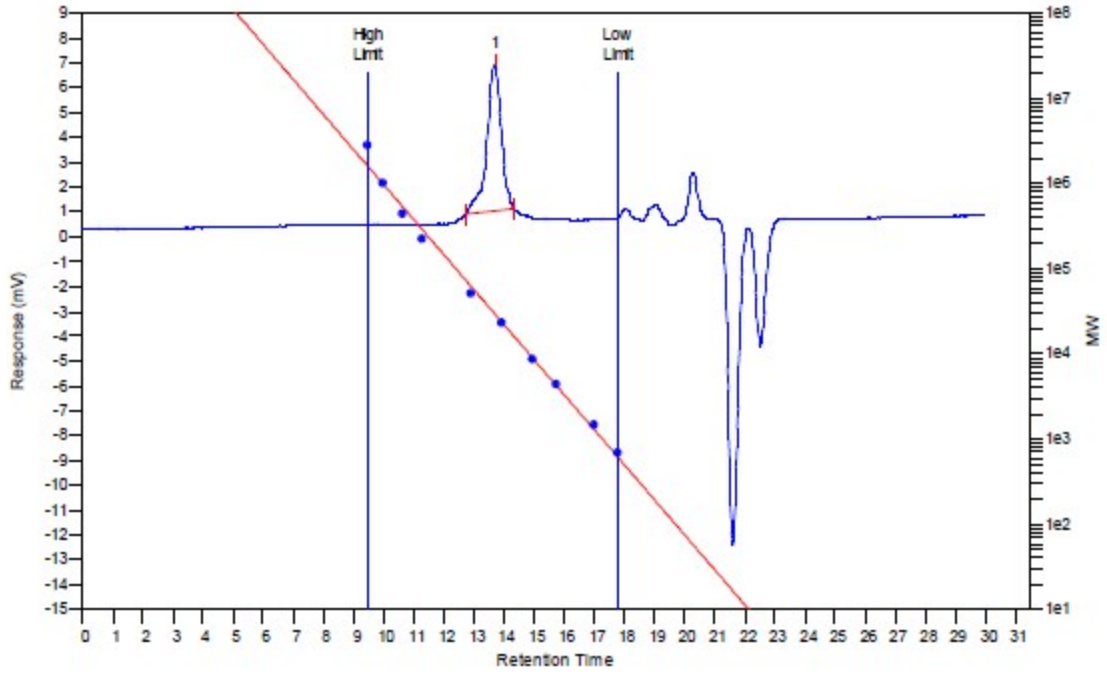

Figure SI47: GPC trace of PLA prepared by bulk polymerisation with Zr(**1**)$_2$ – table 2, entry 3.

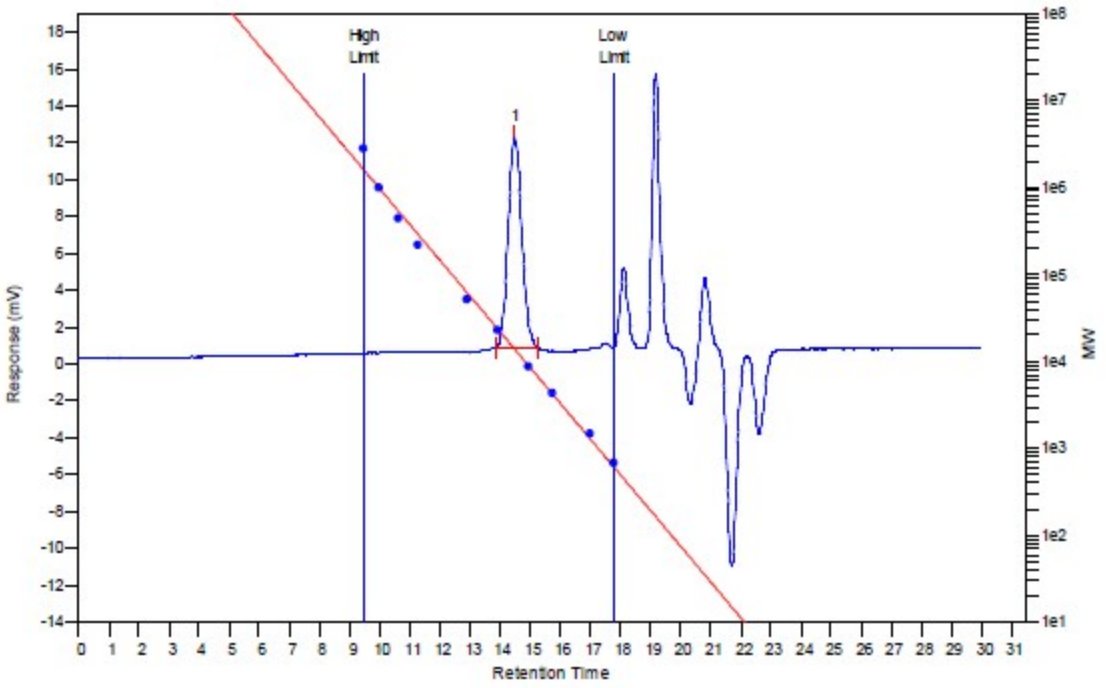

Figure SI48: GPC trace of PLA prepared by solution polymerisation with Hf(**1**)$_2$ – table 2, entry 7.

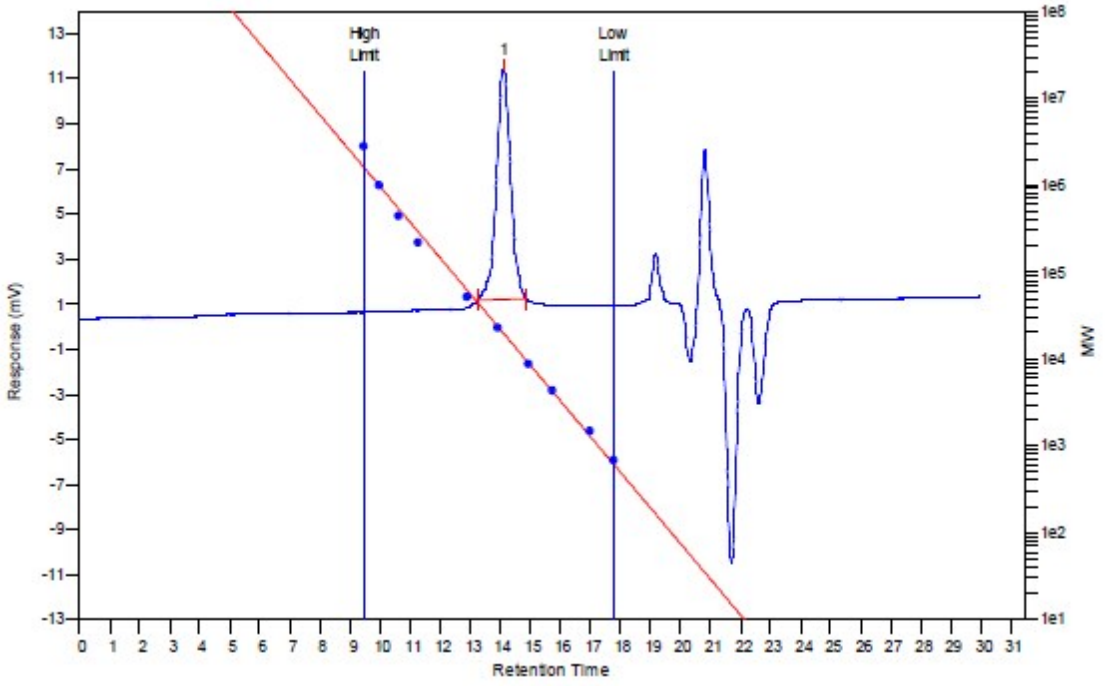

Figure SI49: GPC trace of PLA prepared by solution polymerisation with Al(**9**)Me – table 3, entry 9.

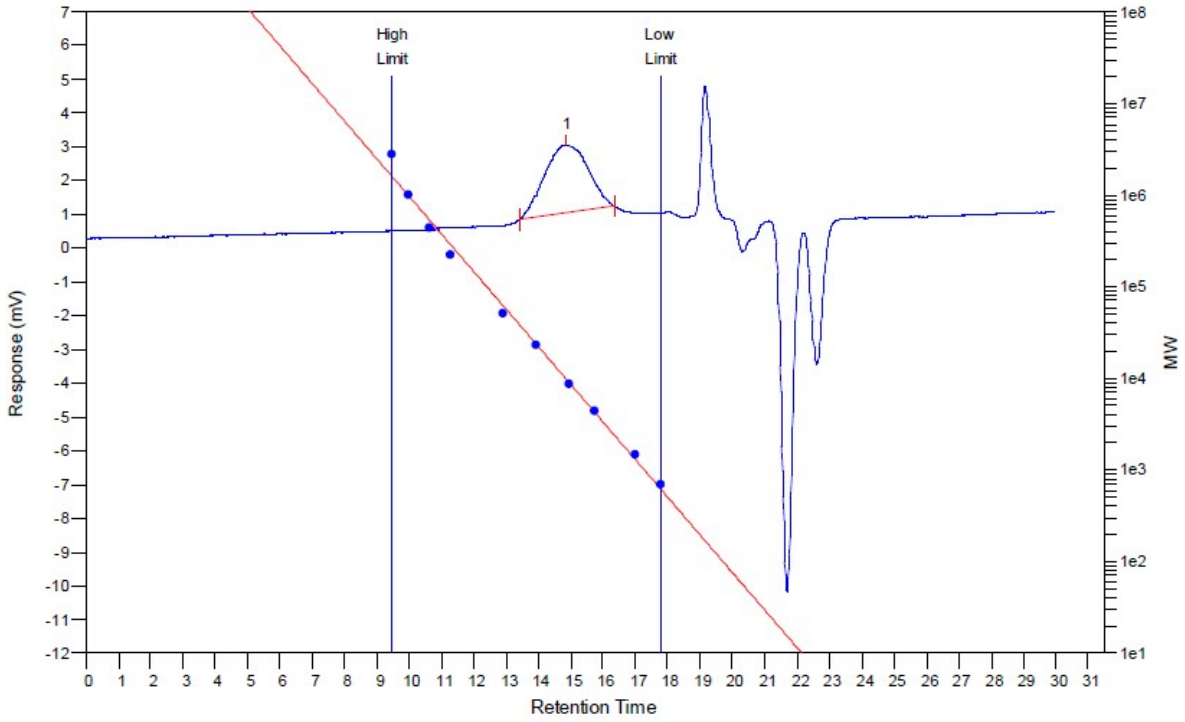

Figure SI50: GPC trace of PLA prepared by bulk polymerisation with **1**H_2

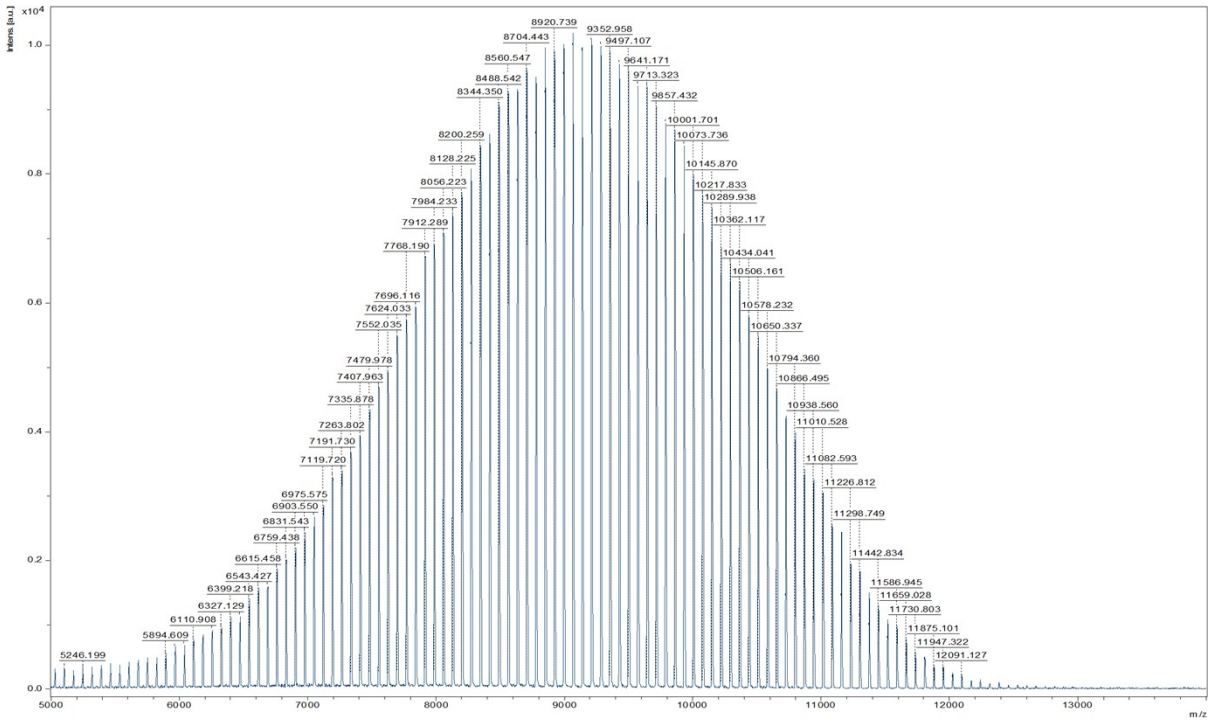

Figure SI51: MALDI-ToF of PLA from solution polymerisation with Zr(**1**)$_2$ - Table 2, Entry 1.

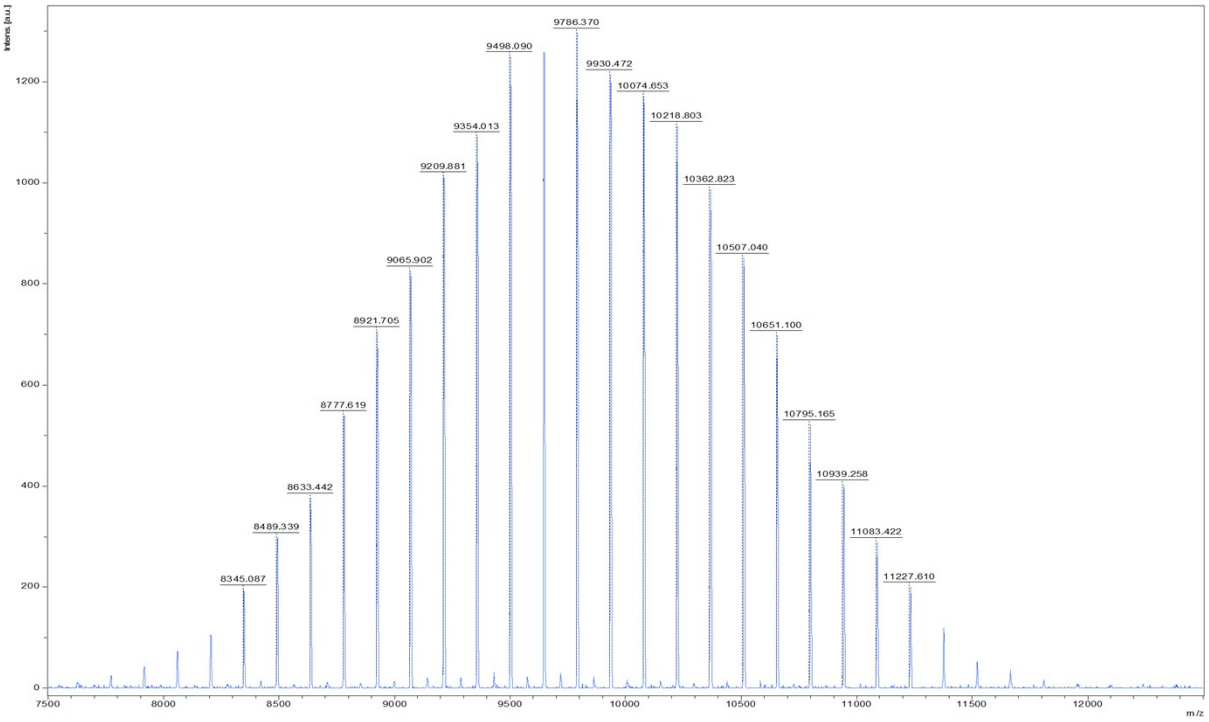

Figure SI52: MALDI-ToF of PLA from solution polymerisation with Al(**2**)Me - Table 3, Entry 2.

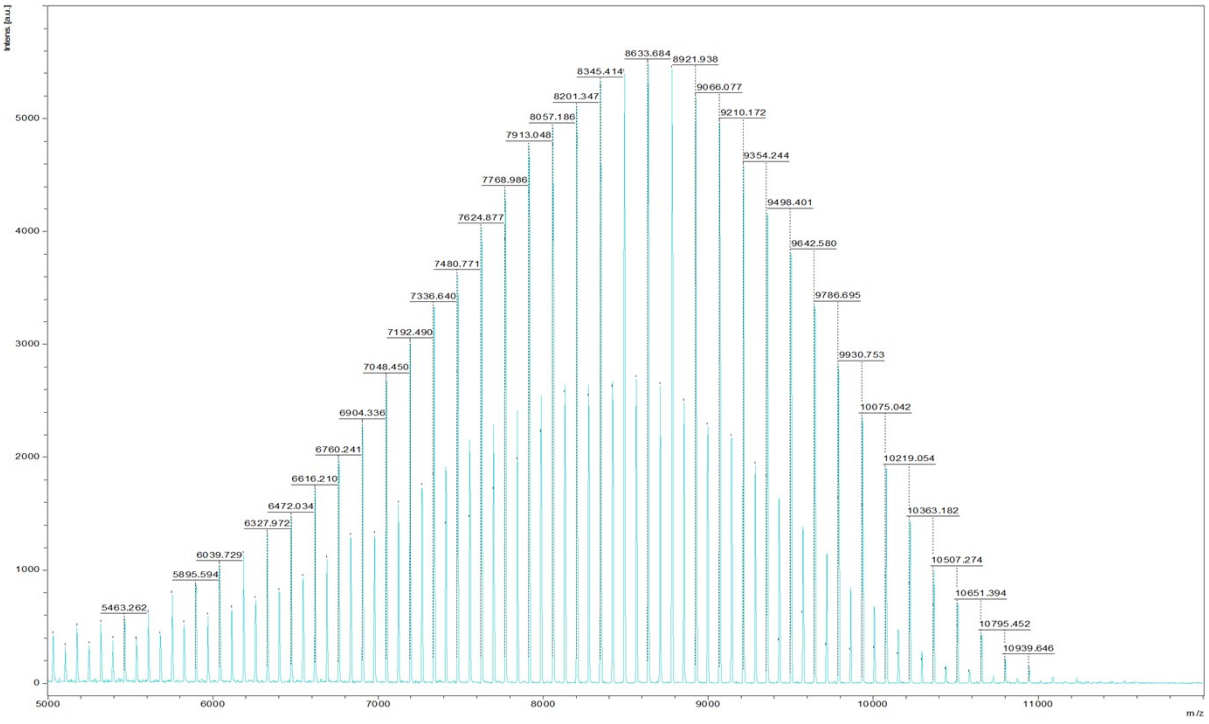

Figure SI53: MALDI-ToF of PLA from solution polymerisation with Al(**4**)Me_2 - Table 3, Entry 4.

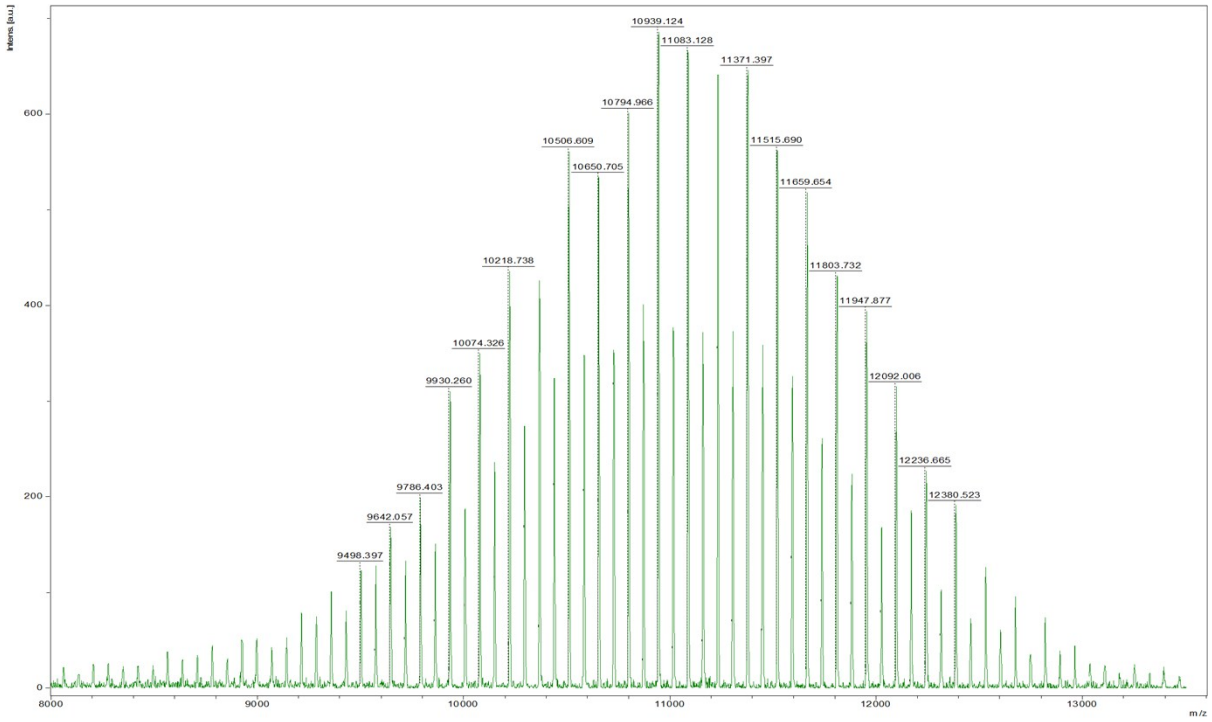

Figure SI54: MALDI-ToF of PLA from solution polymerisation with Al(**7**)Me - Table 3, Entry 7.

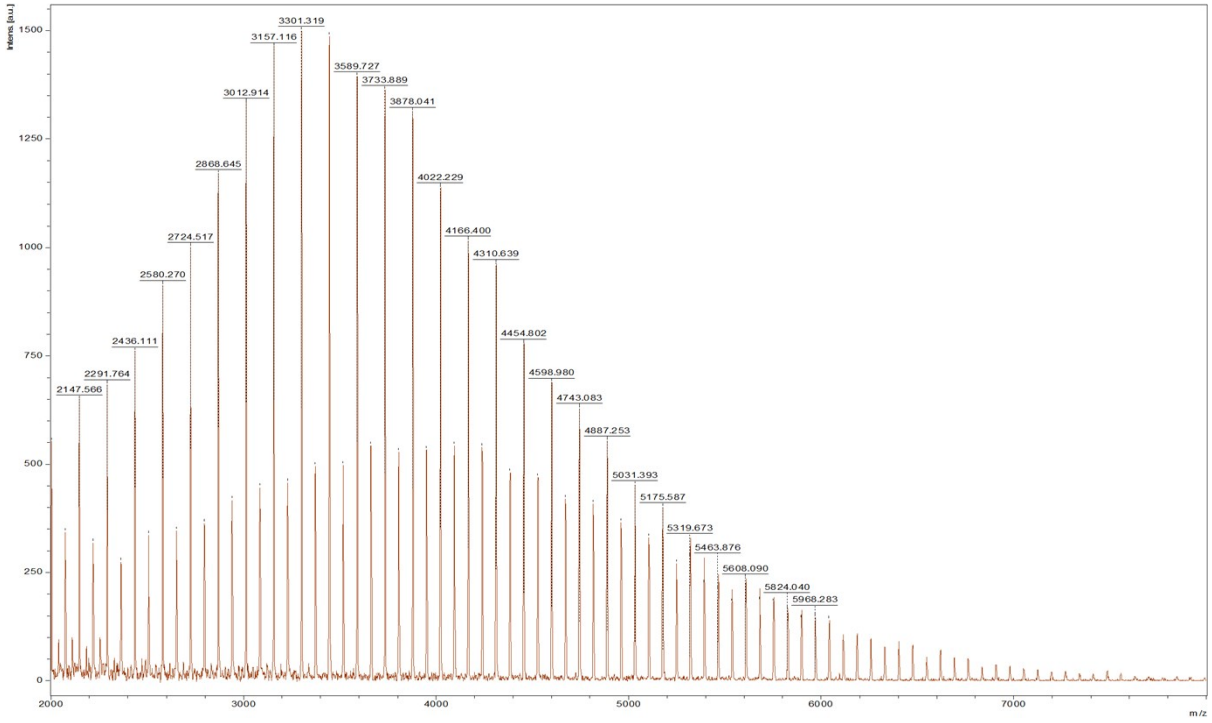

Figure SI55: MALDI-ToF of PLA from bulk polymerisation with **1**H_2.

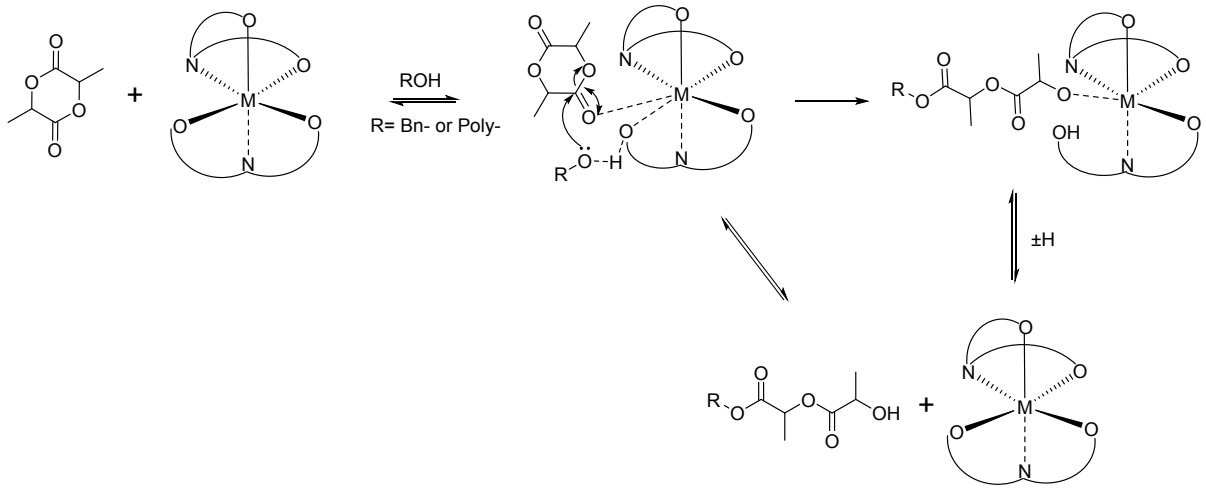

Figure SI56: Schematic to illustrate the potential mechanism for the ROP with the bis-ligated complexes.

Table SI 1: Full X-ray crystallography parameters

Compound reference	**1**H_2	Al(**1**)Me	Al(**2**)Me	Al(**4**)Me_2	Al(**5**)Me_2	Al(**6**)Me_2	Al(**7**)Me	Al(**8**)Me
Chemical formula	$C_{28}H_{38}Cl_2N_2O_2$	$C_{32}H_{46}AlCl_2N_2O_2$	$C_{35}H_{46}AlBr_2N_2O_2$	$C_{23}H_{39}AlN_2O$	$C_{34}H_{54}Al_2N_4O_2$	$C_{26}H_{39}AlN_2O$	$C_{37}H_{57}AlN_2O_2$	$C_{31}H_{45}AlN_2O_2$
Formula Mass	505.50	588.59	713.54	386.54	604.77	422.57	588.82	504.67
Crystal system	Triclinic	Triclinic	Monoclinic	Monoclinic	Monoclinic	Monoclinic	Monoclinic	Triclinic
a/Å	10.7434(9)	8.7940(8)	17.4539(4)	15.1677(3)	19.9805(11)	7.4788(3)	17.6460(7)	8.3422(8)
b/Å	11.2767(11)	12.2980(8)	8.5772(2)	11.97470(10)	8.6659(5)	14.4657(6)	10.2930(5)	9.3504(7)
c/Å	11.9090(11)	15.3990(8)	23.1237(6)	14.1461(2)	20.6358(14)	21.7312(11)	19.4100(8)	19.2341(18)
α/°	85.543(8)	74.378(3)	90	90	90	90	90	100.197(7)
β/°	87.130(7)	87.933(5)	107.060(3)	115.389(2)	107.033(6)	97.752(4)	93.839(3)	101.412(8)
γ/°	70.262(8)	79.786(3)	90	90	90	90	90	94.028(7)
Unit cell volume/Å^3	1353.5(2)	1578.3(2)	3309.42(15)	2321.18(7)	3416.3(4)	2329.53(18)	3517.5(3)	1438.8(2)
Temperature/K	150(2)	150(2)	150(2)	150(2)	150(2)	150(2)	150(2)	150(2)
Space group	*P***Error!**	*P***Error!**	$P2_1/n$	$P2_1/c$	$P2_1/n$	$P2_1/c$	$P2_1/n$	*P***Error!**
No. of formula units per unit cell, *Z*	2	2	4	4	4	4	4	2
No. of reflections measured	12476	33901	28073	27262	14360	4091	30288	8567
No. of independent reflections	6195	7167	8618	4548	6007	4091	6145	8567
R_{int}	0.0212	0.0446	0.0352	0.0381	0.0564	-	0.0845	-
Final R_1 values ($I > 2\sigma(I)$)	0.0398	0.0367	0.0402	0.0391	0.1095	0.0970	0.1175	0.0942
Final $wR(F^2)$ values ($I > 2\sigma(I)$)	0.0916	0.0946	0.0841	0.1008	0.2669	0.2046	0.2944	0.2368
Final R_1 values (all data)	0.0503	0.0465	0.0633	0.0447	0.1477	0.1215	0.1606	0.1234
Final $wR(F^2)$ values (all data)	0.0973	0.1011	0.0926	0.1043	0.2973	0.2156	0.3381	0.2628
Goodness of fit on F^2	1.025	1.061	1.022	1.020	1.041	1.120	1.067	1.076

Compound reference	Hf(**1**)$_2$	Hf(**2**)$_2$	Hf(**3**)$_2$	Ti(**1**)(O^{i}Pr)$_2$	Zr(**1**)$_2$	Zr(**2**)$_2$	Zr(**3**)$_2$
Chemical formula	$C_{30\cdot25}H_{39}Cl_3Hf_{0\cdot50}N_2O_2$	$C_{57\cdot50}H_{75}Br_4Cl_3HfN_4O_4$	$C_{68}H_{100}HfI_4N_4O_4$	$C_{34}H_{49}Cl_2N_2O_4Ti$	$C_{62}H_{86}Cl_4N_4O_4Zr$	$C_{61}H_{84}Br_4N_4O_4Zr$	$C_{62}H_{86}I_4N_4O_4Zr$
Formula Mass	658.23	1490.69	1723.60	668.55	1184.36	1348.18	1550.16
Crystal system	Triclinic	Triclinic	Orthorhombic	Triclinic	Triclinic	Triclinic	Monoclinic
a/Å	10.3949(2)	10.3957(5)	54.9146(5)	10.6236(5)	13.9740(8)	13.8853(9)	19.5802(5)
b/Å	13.7142(3)	13.6050(5)	35.8227(3)	11.1469(8)	14.3110(7)	14.3894(6)	18.0805(3)
c/Å	22.8673(3)	22.9024(11)	13.38270(10)	16.0773(9)	17.2770(6)	17.4919(8)	19.3122(5)
α/°	91.0520(10)	89.912(3)	90	101.894(6)	74.900(3)	74.488(4)	90
β/°	96.1700(10)	84.053(4)	90	102.235(4)	87.307(3)	86.590(5)	108.576(3)
γ/°	109.546(2)	69.887(4)	90	102.233(5)	73.892(2)	74.048(5)	90
Unit cell volume/Å^3	3049.12(10)	3023.2(2)	26326.3(4)	1754.47(19)	3203.6(3)	3237.5(3)	6480.7(3)
Temperature/K	150(2)	150(2)	150(2)	150(2)	150(2)	150(2)	150(2)
Space group	*P***Error!**	*P***Error!**	*Fdd*2	*P***Error!**	*P***Error!**	*P***Error!**	$P2_1/c$
No. of formula units per unit cell, *Z*	4	2	16	2	2	2	4
No. of reflections measured	22737	18821	51826	11314	31292	14806	62477
No. of independent reflections	11721	12294	14439	6173	31292	14806	12703
R_{int}	0.0241	0.0295	0.0337	0.0481	-	0.0205	0.0838
Final R_1 values ($I > 2\sigma(I)$)	0.0329	0.0401	0.0186	0.0749	0.1065	0.0640	0.0529
Final $wR(F^2)$ values ($I > 2\sigma(I)$)	0.0840	0.0945	0.0374	0.2023	0.2707	0.1458	0.1328
Final R_1 values (all data)	0.0333	0.0530	0.0216	0.0798	0.1794	0.1054	0.0639
Final $wR(F^2)$ values (all data)	0.0843	0.1015	0.0377	0.2097	0.3112	0.1685	0.1423
Goodness of fit on F^2	1.061	1.065	0.990	1.036	1.003	1.028	1.018